



**COMPARISON OF MACROBEND LOSSES IN SINGLE MODE
FIBRE (SMF) AND MULTIMODE FIBRE (MMF)**

BY

DORCAS NHIWATIWA

**SUBMITTED IN PARTIAL FULFILMENT OF THE REQUIREMENTS FOR THE
AWARD OF THE DEGREE OF MASTER OF SCIENCE IN APPLIED PHYSICS**

**Supervisor: Dr L. Olumekor
Co-Supervisor 1: Mr. M. Munyaradzi
Co-Supervisor 2: Mr. K. Munjeri**

**DEPARTMENT OF PHYSICS
FACULTY OF SCIENCE
UNIVERSITY OF ZIMBABWE
JANUARY 2012**

In loving memory of my late father
ABISHA SHINGIRAYI NHIWATIWA and dedicated
in tribute to my mum Norah Nhiwatiwa.
For whatever your eye and heart has set on is ATTAINABLE.

ABSTRACT

A comparison of macrobend losses in Single Mode Fibre (SMF) and Multimode Fibre (MMF) is presented. The increased demand on information has seen optical fibres slowly replacing the use of copper coaxial cables for signal transmission, and this, largely due to the high bandwidth and speed of transmission, large carrying capacity and security offered by optical fibres. Signal attenuation however remains a limitation to efficient and quality signal transmission and macrobending is one of the loss mechanisms that contributes to this signal attenuation. Appreciating the responses of the different optic fibres in use to macrobending is therefore instrumental in ensuring macrobending contribution to overall attenuation in optic fibres is minimum at all times. In this study the macrobend losses trends with bending diameter were investigated for the SMF and MMF in similar experimental setups. To do this improvisations were done for a light source using 555 timer astable multivibrator powering a green LED, a light detector using an LDR in a Wheatstone bridge circuit and optic fibres off-cuts. Optic power was measured at the input and output points of the optic fibres using the light detector in bend and straight conditions for determination of signal attenuation in each case. The experimental measurement results show that macrobending losses are more pronounced in a SMF than in a MMF. Characteristic values for macrobending loss are 1268 dB/km for SMF compared to 1155 dB/km for MMF for bending diameter value 4.19 cm. In the SMF macrobending loss trend showed an exponential variation which agrees with work by previous authors. The contribution of macrobending loss in multimode fibre attenuation was however minimal and therefore difficult to quantify. Results also showed that MMF have a higher overall signal attenuation than SMF which justifies the use of SMF in long distance signal transmission. Research findings confirm the significant contribution of macrobending to optic fibre signal attenuation hence the need for careful

consideration in installations for optimal operation of optic fibres. This would mean the choice of optic fibre in any particular instance should consider the high attenuation in MMF not neglecting the insignificant macrobending contribution of MMF to attenuation at any preferred wavelength in order to obtain required transmission characteristics.

Key Words: Macrobending loss, Bending Diameter, Attenuation, Single Mode fibre, Multimode fibre, Optic Fibre.

ACKNOWLEDGEMENTS

I thank the Lord Almighty for such an opportunity, the enablement, the wisdom, the willpower and the strength, for nothing is done without him.

I would like to extend my sincere gratitude to my course coordinator also my supervisor Dr L. Olumekor of the Department of Physics. Sir your commitment, guidance and constructive criticism throughout the research saw me to the completion of this research. I would like to also acknowledge the invaluable contribution I got from my co-supervisors Mr. K. Munjeri of the Department of Physics and Mr. M. Munyaradzi of the Department of Computer Science. Special mention also goes to the Chairman of the Department of Physics Dr E. Mashonjowa and the rest of the teaching staff and technical staff for their overwhelming support and contribution in the realization of this research. To you all, your patience in guiding and mentoring me through the daily paces is greatly appreciated.

To my family and friends, I would like to say thank you for the encouragement, spiritual, moral and financial support, it kept me going. Special mention goes to my mother, for the sleepless nights, the encouragement and for all that could never be expressed in words thank you. I LOVE YOU.

Edwin and Walter together we were a winning team thank you for the advice that was always timely. Itayi the guy who was behind the scenes and who contributed so much for the success of this project, you fought the good fight.

Lastly I would like to acknowledge the initial financial support I received from the University of Zimbabwe, the continued financial support from DAAD throughout my studies and the research grant awarded by the Research Council of Zimbabwe towards carrying out of this research.

LIST OF FIGURES

Fig 2.1: Cross section of a fibre-optic cable.	6
Fig 2.2: Illustration of the Total Internal Reflection principle.....	13
Fig 2.3: TIR in Optic Fibres.....	15
Fig 2.4: Concept of modes in optic fibres.....	19
Fig 2.5: Different loss mechanisms in a typical silica fibre.....	21
Fig 2.6: (a) Microbending; (b) Macrobending.....	26
Fig 2.7: Loss due to microbending and macrobending on basic fibre power loss.....	27
Fig 2.8: Ray field diagram approach.....	29
Fig 2.9: Mode field approach.....	29
Fig 2.10: 555 timer connected for astable operation.....	32
Fig 2.11: LDR light detector circuit.....	33
Fig 2.12: Wheatstone bridge connection and its equivalent circuit.....	34
Fig 3.1: Phototransistor light detector circuit	39
Fig 3.2: Light Detector Circuit.....	40
Fig 3.3: Connection for determining response curve for the two different designs	40
Fig 3.4: Circuit for determining I-V characteristics of an LDR	41
Fig 3.5: Schematic diagram of the experimental set up.....	42
Fig 4.1: Response of Phototransistor 1 to varying light intensity.....	45
Fig 4.2: Response of phototransistor 2 to varying light intensity.....	46
Fig 4.3: Response curve for the LDR	47
Fig 4.4: LDR current voltage characteristics	48
Fig 4.5: $\ln(\alpha)$ (attenuation) vs bend diameter for SMF.....	53
Fig 4.6: $\ln(\alpha)$ (attenuation) vs bend diameter for MMF	53
Fig 4.7: Comparison of Macrobend losses in SMF and MMF	54

LIST OF TABLES

Table 4.1: Single Mode Fibre Measurement Results.....	49
Table 4.2: Attenuation in a single mode fibre.....	50
Table 4.3: Multimode Fibre Measurement Results.....	51
Table 4.4: Attenuation in a Multimode fibre	52

TABLE OF CONTENTS

DEDICATION.....	ii
ABSTRACT.....	iii
ACKNOWLEDGEMENTS.....	v
LIST OF FIGURES.....	vi
LIST OF TABLES.....	vii
CHAPTER ONE: INTRODUCTION.....	i
1.1 Background	1
1.2 Motivation	3
1.2.1 Aim	3
1.2.2 Objectives	3
1.3 Structure of the Thesis.....	4
CHAPTER TWO: LITERATURE REVIEW.....	5
2.1 Introduction	5
2.2 Structure of the Optic Fibre.....	5
2.3 History of Optic Fibres.....	6
2.4 Propagation Phenomena.....	10
2.5 Propagation in Single-mode and Multimode Fibres	16
2.6 Signal Attenuation in Optic Fibres.....	20
2.6.1 Material Absorption.....	23
2.6.2 Scattering	24
2.6.3 Mode coupling and leaky modes	25
2.6.4 Bending Loss	26
2.6.4.1 Microbending	27
2.6.4.2 Macrobending	28
2.7 Light Source	31

2.7.1 Astable Multivibrator	31
2.8 Light Detector	33
2.8.2 Wheatstone bridge theory	34
2.8.3 LDR Theory.....	35
CHAPTER THREE: MATERIALS AND METHODS	36
3.1 Introduction	36
3.2 Materials.....	36
3.2.1 Light Source	36
3.2.2 Light Detector.....	37
3.2.3 Fibre and bending material	37
3.2.4 Additional materials	37
3.3 Method	38
3.3.1 Construction of a light source circuit	38
3.3.2 Construction of light detector circuit.....	38
3.3.2.1 Phototransistor Light detector circuit.....	39
3.3.2.2 LDR light detector circuit	39
3.3.3 Measurements	41
3.3.3.1 Measurements with Single Mode Fibre	41
3.3.3.2 Measurements with Multimode fibre.....	42
3.4 Precautions	42
3.5 Sources of Errors	43
CHAPTER FOUR: RESULTS AND DISCUSSION	45
4.1 Introduction	45
4.2 Phototransistor Response	45
4.3 LDR Characterisation.....	47
4.3.1 LDR Response.....	47
4.3.2 Current Voltage characteristics of LDR	48
4.4 Measurements with Single Mode Fibre	49
4.4.1 Calculation of Attenuation.....	50
4.5 Measurements with Multimode Fibre	51

4.5.1 Calculation of Attenuation in Multimode Fibre	52
CHAPTER FIVE: CONCLUSION AND RECOMMENDATIONS	56
5.1 Introduction	56
5.2 Conclusion.....	56
5.3 Recommendations	57
REFERENCES.....	58
ACRONYMS and ABBREVIATIONS	62
APPENDICES	63
Appendix 1: Phototransistor 1 response raw results	63
Appendix 2: Phototransistor 2 response raw results	63
Appendix 3: LDR Response raw results	64
Appendix 4: Current Voltage Characteristics of LDR	64
Appendix 5: Bend Diameter Measurements	65
Appendix 6: Measurements for the single mode fibre	65
Appendix 7: Measurements for the multimode fibre	Error! Bookmark not defined.

CHAPTER ONE: INTRODUCTION

1.1 Background

Optic fibres have played a major role in the revolution witnessed in the telecommunication industry in the recent years. An optic fibre operating at 10 Gbit/s for example can handle over 130,000 simultaneous voice channels compared to about 2000 voice channels that can be carried by one of the best copper coaxial cables [1, 2]. Information and data use has become so widespread across all ages in developed and developing countries. This has been made possible by the continued reduction of cost for accessing such services aided by the increased use of optic fibres for signal transmission.

An optic fibre is a long thin strand of very pure glass about the diameter of hair that acts as a waveguide making use of light for the propagation of signals through it from one point to the other [3]. Optic fibres are usually installed underground for long distance transmission and due to the nature of terrain at times it is inevitable that the cables are bend. A basic single optic fibre is made up of the core whose diameter ranges from 8 to 62.5 μm and is a thin glass centre of the fibre where the light travels, the cladding of diameter 125 μm which is the outer optic material surrounding the core reflecting light back into the core and lastly the buffer coating with diameter ranging 250 μm to 900 μm . The buffer coating is a plastic coating that protects fibre from moisture and damage [3, 4]. The optic fibre sometimes has a strengthening member and an extra protective coating. Light propagation is through Total Internal Reflection (TIR) made possible by the different refractive indices possessed by the

core made of higher refractive index material and cladding made of lower refractive index material.

There are three major types of optic fibres namely multimode fibres (MMF), single mode fibre (SMF) and plastic optic fibre (POF). Optical fibres have found wide usage in telecommunication, sensor and medical systems therefore signal propagation (light) with minimum attenuation/power loss is important for efficient use of fibres in the several application fields.

Light propagating in an optic fibre is attenuated due to the various loss mechanisms present in the optic fibre system. Attenuation is defined as the reduction or loss of power of a signal as it propagates along a medium. The overall attenuation in an optic fibre is the sum of signal power losses due to absorption, scattering, micro bending, macrobending and other loss mechanisms [4]. It is measured in decibels/kilometre, and is also known as the attenuation coefficient or attenuation rate [4].

Continuous research and development has managed to significantly reduce the overall attenuation of signals in optic fibres. Macrobending is one of the loss mechanisms resulting in power loss. It is therefore important to characterise macrobend losses for different bend diameters, types of optic fibre material and wavelengths of signals so that choice of optic fibre in any application is done such that the contribution of loss due to macrobending is minimised. This study will concentrate on attenuation due to bending particularly macrobending. Macrobends are defined as bends on a fibre whose radius of curvature/bend diameter is large relative to the fibre diameter that is $R \gg a$ where a , denotes the core radius and R , the radius of curvature [5, 6].

1.2 Motivation

There continues to be research and development aimed at reducing signal attenuation in optic fibres. This has a direct bearing on the overall cost of using optic fibres as a means of transmission as well as optimizing their performance in their conditions of operation. Most of the research work has been carried out independently either for SMF or MMF [6, 7, 8, 9]. It is therefore the intention of this study to investigate on the macrobend losses in both single mode fibre and multimode fibre subjected to similar experimental conditions. The study hopes to establish differences in the macrobending losses excluding the differences in experimental setups and attribute any observed differences to the structure and properties of these fibres. In view of this background the aim and objectives of this research are outlined below.

1.2.1 Aim

It is the aim of this research to compare macrobending losses in SMF and MMF systems when investigated under similar experimental setups.

1.2.2 Objectives

- i) To verify and isolate attenuation due to other loss mechanisms for example scattering and absorption
- ii) To calculate signal power loss due to macrobending in SMF and MMF.

- iii) To establish relationship between bending loss and bend diameter for,
 - a) SMF,
 - b) MMF
- iv) To compare the bending loss trends in the two optic fibre systems.

1.3 Structure of the Thesis

Chapter 1, is a brief introduction to Optical fibres and the power loss due to macrobending in optical fibres. It also outlines the objective of the thesis/study.

Chapter 2, gives a detailed literature review on the basics about optical fibres and signal attenuation in optical fibres. Macrobend loss trends with bending diameter, angle and wavelength are discussed with reference to previous work done by other scholars.

Chapter 3, details the materials and methods used in carrying out the research. It also describes the design and construction of the light source and detector circuits.

Chapter 4, Presentation of raw data, analysis and discussion of obtained results;

Chapter 5, concludes on the research work based on findings in comparison to objectives and previous work. Recommendations are also made for further work.

CHAPTER TWO: LITERATURE REVIEW

2.1 Introduction

This chapter gives a brief description of the structure, history and operation of optical fibres. Loss mechanisms that contribute to reduction in signal power as the signal propagates along the length of the fibre are discussed. The chapter further explores macrobend losses in both SMF and MMF and work that have been done by other researchers.

2.2 Structure of the Optic Fibre

An optical fibre strand (cable) is made up of the following components as shown in figure 2.1;

- a) Optic core – thin glass at the centre responsible for carrying light signals. It is commonly made of germania and silica.
- b) Optic cladding – outer optic material surrounding the core that reflects light back into the core. It is made of pure silica.
- c) Buffer coating – plastic coating (shielding) that protects fibre from damage and moisture.
- d) A strength member - material surrounding the buffer preventing stretch when the fibre is being pulled [10].
- e) Outer jacket – added to protect against abrasion, solvents and other contaminants.

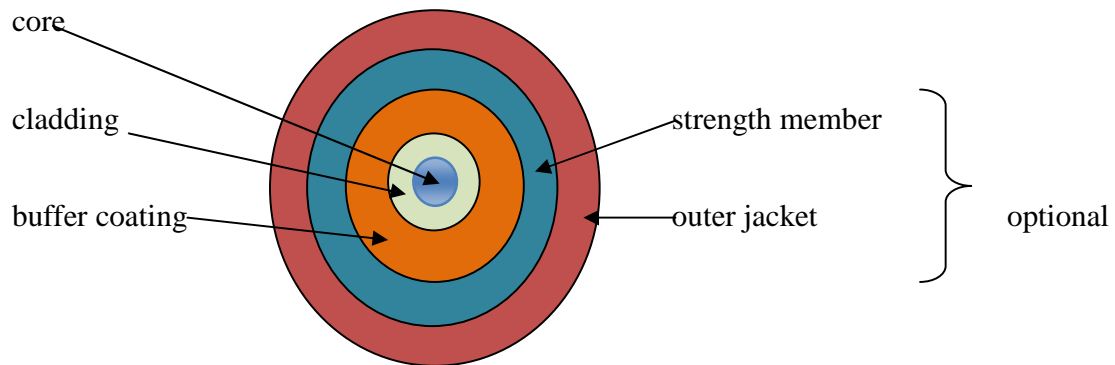


Fig 2.1: Cross section of a fibre-optic cable.

2.3 History of Optic Fibres

The use of optic fibre was generally minimal until in 1970s when Corning Glass Works was able to produce a fibre with a loss of 20 dB/km. It was recognized that optic fibre would be feasible for telecommunication transmission only if glass could be developed so pure that attenuation would be 20 dB/km or less. Further improvements in the structure and composition of the optic fibre has helped reduce this loss to about 0.2 - 0.3 dB/km [11]. Fibre optic systems find application in various industrial fields.

Some of the fibre optic system applications are;

- i) Sensor systems for the measurement of pressure, temperature, sound, vibration, linear and angular position, strain, humidity, viscosity changes and ruptures. Optic fibre sensors make use of properties of light among them, the wavelength, intensity, phase and spectral composition where the measurand modulates the light in the

optic fibre and the change in light properties becomes the measure for the temperature, position and so on [12].

- ii) The fibre optic gyroscope being developed for aircraft and spacecraft- the Fibre Optic Gyroscope (FOG) is a rotation or rotation rate sensor comprising of up to three optic fibre coils one for each of the degree of freedom required. Light is launched into both ends of each coil simultaneously and recombined at a detector. The light propagating into a coil that experiences rotation will undergo Doppler-shift also known as Sagner Effect resulting in the counter propagating beams recombining out of phase. The interference pattern resulting thereof is analysed to determine degree and rate of rotation [13].
- iii) Measurement of electric field and electron density (for example in mines without introducing electric currents).
- iv) Medical Industry –an example of use of Optical fibres has been in laproscopic surgery (or more commonly, keyhole surgery), which is usually used for operations in the stomach area such as appendectomies. Keyhole surgery usually makes use of two or three bundles (each bundle containing about thousands of fibres) of optical fibres. Each of the bundles serves a purpose having the advantage of small incisions than would be in normal surgery. Operating instruments can be introduced in the target area with one bundle, with another bundle of optical fibres being used for illumination of the chosen area, and the other bundle can be used to bring

information back to the surgeon (that is imaging). This can be coupled with laser surgery, by using an optical fibre to carry the laser beam to the relevant spot, which would then be able to be used to cut the tissue or affect it in some other way [14].

The use of optical fibres in the several application fields discussed above is largely because of their light weight, small size, resistance to electromagnetic interference, wide bandwidth and environmental ruggedness [15].

Attention and most of the research work has been directed towards the use of optical fibres in the telecommunications field and as such fibre optic cables are slowly replacing the use of copper coaxial cables as a means for communication and signal transmission. Some of the advantages of optical fibres over coaxial copper cables are highlighted below;

- i) Large bandwidth – light the carrier of information in the optical waveguide, is an electromagnetic radiation having a frequency around $4 - 8 \times 10^{14}$ Hz. Since the information carrying capacity of a transmission system is directly proportional to the carrier frequency of the transmitted signals the optical fibre yields greater transmission bandwidth than the conventional communication systems for which radio wave frequency is about 10^6 Hz and microwave frequency is about 10^{10} Hz.
- ii) Low loss – through research and development, transmission loss in optic fibres has been significantly reduced down to 0.2 dB/km [16, 11]. In modern optical fibre telecommunication systems, fibres having a transmission loss of 0.002 dB/km are now being used and the section that can be covered without needing a repeater can

exceed 100 km (signals can be sent up to 100 times further along optical fibres than along copper cables without the need for intermediate amplifiers). The use of erbium-doped silica fibres as optical amplifiers means distortion produced during signal strengthening is minimized since the amplification is done within the optical domain [11].

- iii) Security – signals being transmitted in an optic fibre do not radiate (electrical or magnetic energy) and so cannot be tapped easily.
- iv) Interference- optical fibres are not susceptible to electromagnetic interference, thus there is no cross-talk between adjacent fibres bundled together in an optical cable. They are also not susceptible to radio frequency interference and voltage surges hence their application in explosive environments.
- v) Speed of transmission – data transfer rates are high and are in the order of several Mbit/s to Gbit/s.

There are three basic types of optic fibres namely single mode fibre (SMF), multimode fibre (MMF) and plastic optic fibres (POF). These fibres can either be a step index fibre or graded index fibre, but the SMF is limited to a step index profile. A step index fibre is one whose refractive index of the core is uniform throughout and undergoes an abrupt or step change at the core cladding boundary, whereas the graded index fibre has the core refractive index varying in a parabolic manner with the maximum value of the refractive index being at the centre of the core [17]. Single mode fibres have a core diameter that is between 8 -10 μm and

has one mode of transmission. They usually operate in the 1310 nm and 1550 nm wavelength regions. SMF requires a light source with a narrow spectral width and lasers can serve that purpose [18].

Multimode fibres have a larger core diameter which can either be 50 or 62.5 μm , transmitting at 850 nm and 1300 nm region of wavelengths. LEDs are used as the light source. A newer type of fibre is the plastic optic fibre made from plastic materials such as polymethyl methacrylate PMMA with refractive index n , ($n = 1.49$), polystyrene ($n = 1.59$), polycarbonates ($n = 1.5 - 1.57$), fluorinated polymers and so on. Plastic Optic fibres have a larger core diameter around 1mm. They are more durable and more flexible than glass fibre. Single Mode fibres are mostly used for long distance transmissions while MMF are used for in-house/LAN installations that is short distance transmissions and the choice for the use of these optic fibres has been greatly influenced by their cost and performance.

2.4 Propagation Phenomena

The propagation of light in optic fibres is best understood by considering the electromagnetic (EM) field theory and the interaction of an EM field at an interface between two dielectric media. Considering an EM wave that is incident on an interface of two dielectric media, its EM field is made up of two components, namely the electric and magnetic intensity vectors:

$$\mathbf{E}_o = E_o^o e^{-i(\omega t - k_o r)} \quad 2.1$$

$$\mathbf{H}_o = \frac{n_o}{k_o} k_o \times \mathbf{E}_o \quad 2.2$$

where r = the position vector for an arbitrary point in space

ω = the radian frequency of the EM wave

n = refractive index

k_i = propagation vector ($i = 0, 1, 2$)

E_i^0 = amplitude for electric intensity vector ($i = 0, 1, 2$)

t = time

From equation 2.1 it is seen that the amplitude of E_0 is time independent and its direction is tangential to the direction of propagation. The direction of propagation of the field is given by the propagation or wave vector k_0 and its direction is normal to that of the wave front.

From equation 2.1 and 2.2 one can define a term;

$$|k| = \omega \left(\frac{n}{c} \right) \quad 2.3$$

where c = is the speed of light

On meeting the interface between the two media the incident wave is reflected and refracted or transmitted, and the forms of the reflected and transmitted waves can be expressed as was done for the incident wave.

The reflected wave is given by:

$$E_1 = E_1^0 e^{-i(\omega t - k_1 r)} \quad 2.4$$

$$H_1 = \frac{n_1}{k_1} k_1 \times E_1 \quad 2.5$$

while the transmitted wave can be expressed as,

$$\mathbf{E}_2 = E_2^0 e^{-i(\omega t - k_z z)} \quad 2.6$$

$$\mathbf{H}_2 = \frac{n_2}{k_z} k_2 \times \mathbf{E}_2 \quad 2.7$$

Maxwell summarises the empirical and mathematical investigations by other scientists, Ampere, Faraday and Gauss into a set of equations or laws that helps in understanding what happens at the boundary of the two dielectric media [10]. The application of Gauss's law at a dielectric boundary tells us that the normal (that is the perpendicular) component of the electric field is continuous across the boundary and expressed mathematically it gives the relationship:

$$(\epsilon_2 \mathbf{E}_2 - \epsilon_1 \mathbf{E}_1) = 0 \quad 2.8$$

where ϵ is the permittivity of free space, \mathbf{E} is the electric field intensity and \mathbf{B} the magnetic induction.

The other set of Maxwell's equations are expressed as follows:

$$\frac{\partial \mathbf{B}}{\partial t} = 0 \quad 2.9$$

$$\nabla \times \mathbf{E} = 0 \quad 2.10$$

Evaluating equation 2.9 and 2.10 using Stokes theorem and performing an integral over the perimeter of a bounding area leads to another boundary condition for the electric field tangential components. The components must be continuous across the boundary between the two media. Similarly, noting that there is no divergence to a magnetic field,

$$\nabla \cdot \mathbf{B} = 0 \quad 2.11$$

$$(\mathbf{B}_2 - \mathbf{B}_1) \cdot \mathbf{n} = 0 \quad 2.12$$

Interpretation of equation 2.12 shows that the tangential components of the magnetic induction vector, \mathbf{B} , are also continuous across this dielectric boundary [10].

$$n_1 > n_2$$

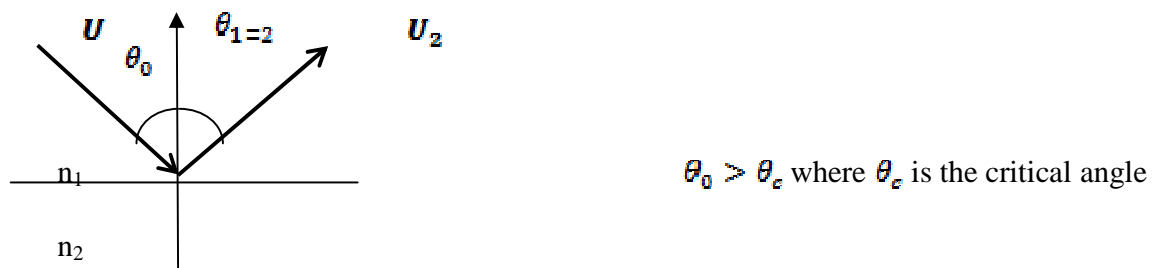
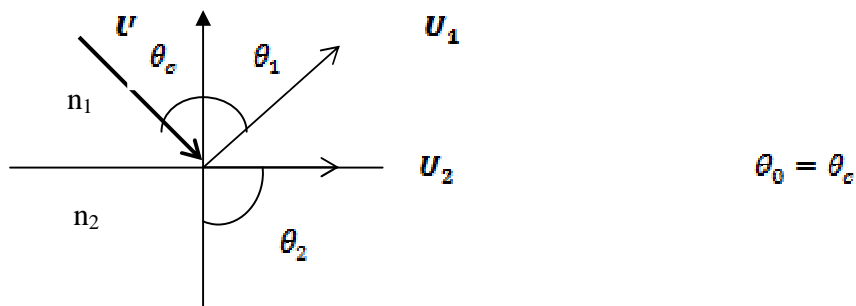
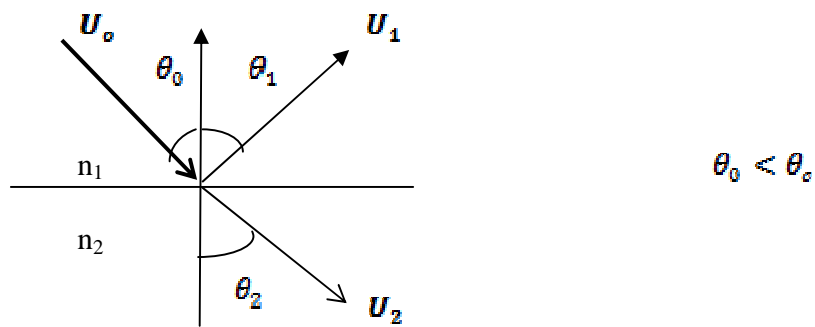


Fig 2.2: Illustration of the Total Internal Reflection principle

From Figure 2.2 all the wave vectors are in the plane of incidence or coplanar which gives the following equalities;

$$k_o \sin \theta_o = k_1 \sin \theta_1 = k_2 \sin \theta_2 \quad 2.13$$

Total Internal Reflection means that the reflected wave and the incident wave are in the same medium that is

$$k_o = k_1 \text{ or } \theta_o = \theta_1 \quad 2.14$$

Applying this to equation 2.3, then

$$\frac{k_1}{n_1} = \frac{k_2}{n_2} \quad 2.15$$

$$\text{From which } n_1 \sin \theta_o = n_2 \sin \theta_2 \text{ (Snell's law)} \quad 2.16$$

When $\theta_2 = \pi/2$ (meaning the refracted angle =90°), then Snell's law can be rewritten as:

$$\sin \theta_o = \frac{n_2}{n_1} \quad 2.17$$

As the sine of a non-imaginary angle can never be greater than one, it requires that $n_1 \geq n_2$.

The incident angle at which $\theta_2 = \pi/2$ is the critical angle θ_c . Any other light incident at an angle greater than θ_c will result in $\theta_2 > \pi/2$ such that no light will be transmitted, as k_2 points along the boundary itself.

Light has to be introduced at the core-cladding interface of an optic fibre at an angle greater or equal to the critical angle which is equal to the acceptance angle of the fibre for it to be guided along the dielectric waveguide. If the angle of the input EM wave is larger than the

acceptance angle, then incident light will not be totally internally reflected but will enter the cladding, causing it to glow. Confinement of light in the core of a fibre is through a series of reflections that is total internal reflection at the core-cladding interface.

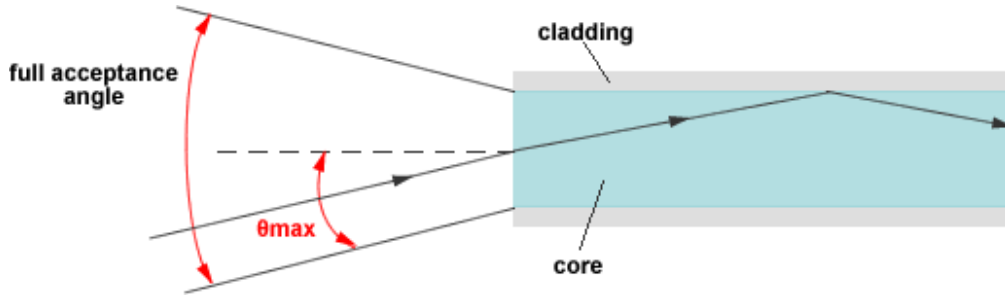


Fig 2.3: TIR in Optic Fibres

The full acceptance angle forms what is known as the acceptance cone of the fibre. Half-angle of this cone is the acceptance angle, θ_{max} . The acceptance angle can be determined from the respective refractive indices of the cladding and core and is also related to the Numerical Aperture of the optic fibre.

$$NA = n \sin \theta_{max} = \sqrt{n_f^2 - n_c^2} \quad 2.18$$

where n is the refractive index of the medium where light is travelling before entering the fibre,

n_f the refractive index of the fibre core and n_c the refractive index of the cladding[19].

2.5 Propagation in Single-mode and Multimode Fibres

Analysis of propagation is made simple by assuming the cladding to be of infinite extent, that is the cladding diameter is large enough for the propagating field to decay to a negligible level at its outer edge. The description of the modal fields is also based on the weakly-guiding approximation where $n_1 - n_2 < n_1$. The approximate mode solutions derived in this way are very nearly polarized and are denoted by $LP_{v\mu}$ where v and μ denote the zeros of the field in the azimuthal and radial directions respectively. The linearly polarized modes correspond to a superposition of the two modes $HE_{v+1,\mu}$ and $HE_{v-1,\mu}$ of the exact solution of Maxwell's equations. The exact modes are nearly degenerate and as n_2 approaches n_1 their propagation constants become identical. Maxwell's equations with the weakly-guiding approximation give the scalar equation as:

$$\frac{d^2\psi}{dr^2} + \frac{1}{r} \frac{d\psi}{dr} + \frac{1}{r^2} \frac{d^2\psi}{d\phi^2} + [n^2(r)k^2 - \beta^2]\psi = 0 \quad 2.19$$

where ψ is the field (\mathbf{E} or \mathbf{H}), $k = 2\pi/\lambda$ is the free-space wave number, $n(r)$ is the radial variation of the refractive index and r, ϕ are the cylindrical co-ordinates. The propagation constant β of a guided mode obviously lies between the limits $n_2k < \beta < n_1k$. The fibre is circular in cross-section and the solutions of the wave equation are separable, having the form:

$$\psi = E(r) \cos v\phi e^{j(\omega t - \beta z)} \quad 2.20$$

In single-mode fibres only the fundamental LP_{01} mode propagates and has no azimuthal dependence, that is $v=0$. It corresponds to the HE_{11} mode derived from the exact analysis, and the fundamental equation reduces to

$$\frac{d^2 E}{dr^2} + \frac{1}{r} \frac{dE}{dr} + [n^2(r)k^2 - \beta^2]E = 0 \quad 2.21$$

For the step-index fibre, the one with a constant refractive index n_1 in the core, equation 2.21 is the Bessel's differential equation and the solutions are cylinder functions. The field must be finite at $r = 0$ and therefore in the core region the solution is a Bessel function, J_v . Similarly the field must vanish as $r \rightarrow \infty$ so that the solution in the cladding is a modified Bessel function, K_v . For the fundamental LP_{01} mode polarized in either x or y direction, the field is therefore:

$$E(r) = AJ_0(UR) \quad R < 1 \quad (\text{core}) \quad 2.22(a)$$

$$= AJ_0(U) \frac{K_0(WR)}{K_0(W)} \quad R > 1 \quad (\text{cladding}) \quad 2.22(b)$$

where $R = r/a$ is the normalized radial co-ordinate and A is the amplitude co-efficient. U and W are the Eigen values in the core, and cladding respectively and are defined by:

$$U^2 = a^2(n_1^2 k^2 - \beta^2) \quad 2.23$$

$$W^2 = a^2(\beta^2 - n_2^2 k^2) \quad 2.24$$

and by adding 2.23 and 2.24 we get,

$$U^2 + W^2 = a^2 k^2 (n_1^2 - n_2^2) \quad 2.25$$

These parameters are related to the normalized propagation constant b , defined as

$$b = \frac{[(\beta/k) - n_2^2]}{2n_1^2 \Delta} = 1 - \frac{U^2}{V^2} \quad 2.26$$

$$\text{Where } \Delta = \frac{n_1^2 - n_2^2}{2n_1^2} \approx \frac{n_1 - n_2}{n_1} \ll 1 \quad 2.27$$

The limits of β are $n_1 k$ and $n_2 k$ for a guided mode, so that $0 \leq b \leq 1$. Normalising the field expressions in equation 2.21 so that they have the same value at $r = a$, and also considering that the tangential electric field components must be continuous at this point, the following eigen value equation for LP_{01} is obtained:

$$\frac{U J_1(U)}{J_0(U)} = \frac{W K_1(W)}{K_0(W)} \quad 2.28$$

The Eigen value, U and hence β can be calculated as a function of the normalized frequency by solving equations 2.26 and 2.28. At the lower limit of $\beta = n_2 k$ the mode-phase velocity equals the velocity of light in the cladding and is no longer guided. The mode is cut off and the Eigen value $W = 0$. As β increases, less power is carried in the cladding and at $\beta = n_1 k$ all the power is confined to the core. The limit of single-mode operation is determined by the wavelength at which the propagation constant of the second, LP_{11} , mode equals $n_2 k$ and for a step-index fibre this cut-off condition is given by $J_0(V_c) = 0$ where V_c denotes the cut-off value of V which, for the LP_{11} mode, is equal to 2.405. The fundamental mode has no cut-off and hence the single-mode operation is possible for $0 \leq V \leq 2.4$ [20]. The V -number is the normalised optical frequency and it determines the fraction of the optical power in a certain mode which is confined to the fibre core.

In multimode fibres power is launched into a large number of modes having different spatial field distributions, propagation constants, and chromatic dispersion. A mode in optics is defined as the way the wave travels through space or it can simply be defined as the

distribution of light energy across the fibre. Mathematically modes are solutions for the wave propagation of light taking into consideration Maxwell's equations and appropriate boundary conditions. The concept of modes in optic fibres is illustrated in the diagram Figure 2.4.

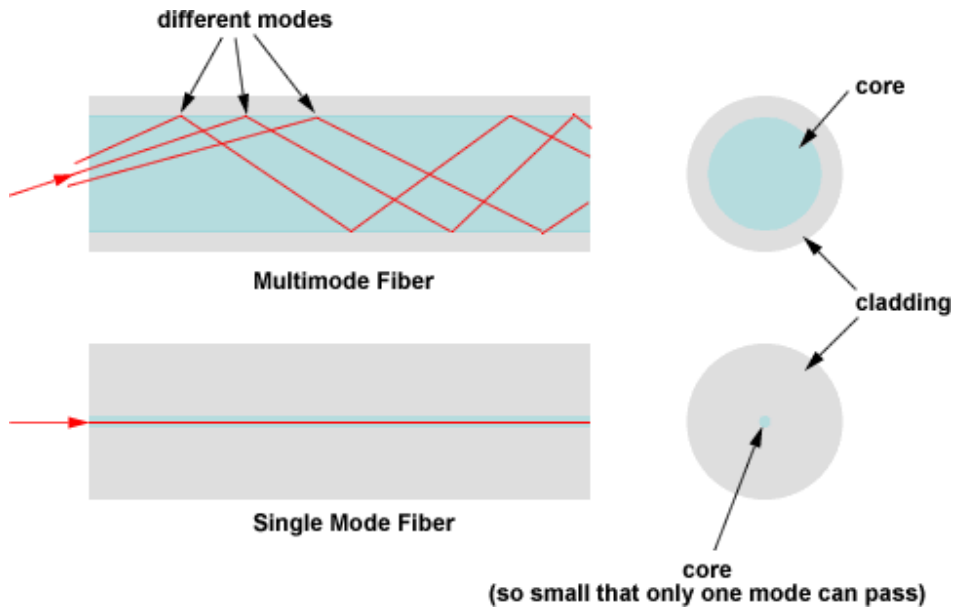


Fig 2.4: Concept of modes in optic fibres.

The V number is greater than 2.405 in multimode fibres and the total number of modes N propagating through a given multimode step index fibre is given by;

$$N_m = \frac{V^2}{2} \approx 0.5 \left(\frac{\pi D \times (NA)^2}{\lambda} \right) \quad 2.29$$

where D is the core diameter, λ is the operating wavelength and NA is the numerical aperture (or acceptance angle). For a multimode graded index profile having a parabolic refractive index profile N_m is given by:

$$N_m = \frac{V^2}{4} \quad 2.30$$

equal to half the number supported by a multimode step index fibre.

2.6 Signal Attenuation in Optic Fibres

Attenuation of signals is a crucial quantity that should be considered in optic fibre communication. This is because it is a determining factor of cost of fibre optic telecommunication systems as it determines spacing of repeaters needed to maintain acceptable signal levels. This ensures quality and correct delivery of signals at the receiving end. The overall attenuation pattern, a sum of attenuation contributed by the various loss mechanisms in Figure 2.5 gives a quite different attenuation pattern than would be ideally expected of a damped exponential. The deviation is due to the fact that attenuation in optic fibres is dependent on both fibre properties and structure. The attenuation is also found to be dependent on the transmission characteristics of the signal, for example wavelength.

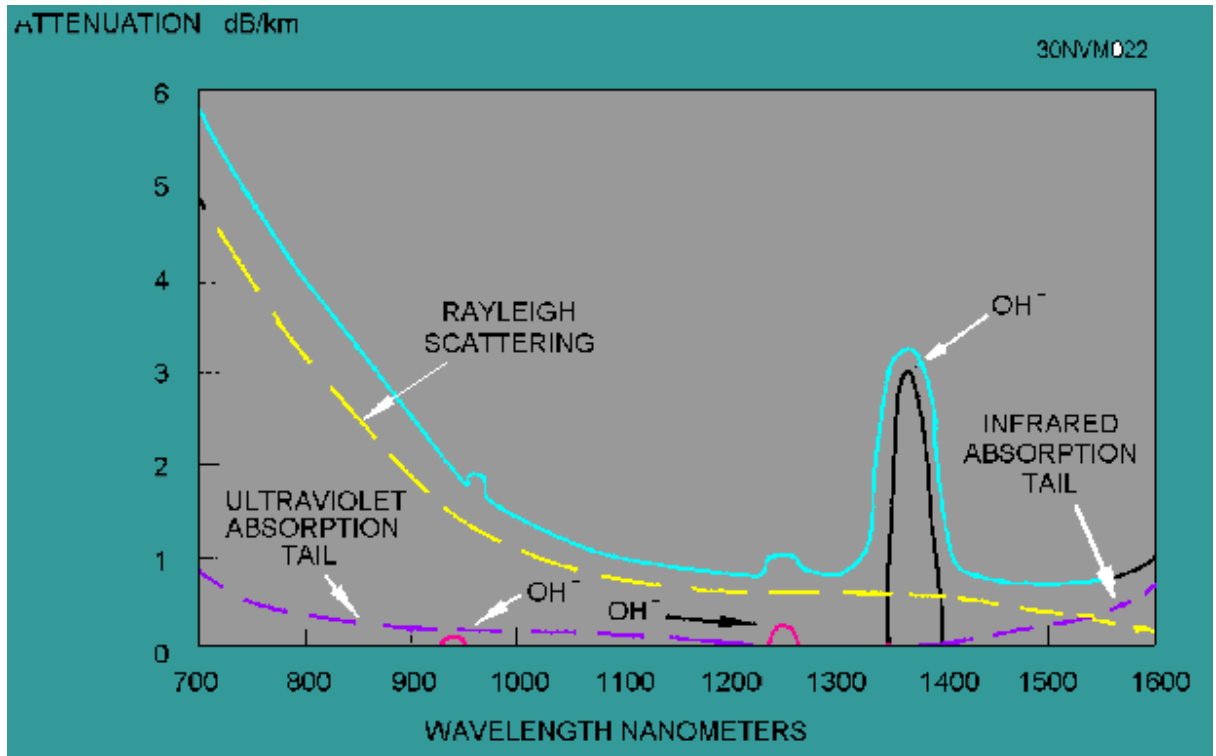


Fig 2.5: Different loss mechanisms in a typical silica fibre

Attenuation is a relative measure of the output to input intensity and is given by.

$$\text{Attenuation (dB/km)} = \frac{10}{L} \log \left(\frac{I_o}{I_i} \right) \quad 2.31$$

where I_o = the measured output power,

I_i = the reference input power and

L = the length of the optic fibre [21].

Optical input power is the power injected into the fibre from the optical source and the optical output power is the power received at the fibre end [22]. The power losses and other characteristics of the fibre can be measured with instruments such as an Optical Power Meter or an Optical Time-Domain Reflectometer (OTDR).

Normally most of propagating energy is contained in the core but there is always a radially decaying evanescent field in the cladding, which may extend over several wavelengths in the case of single-mode fibres. Both core and cladding materials must therefore have very low absorption and scattering losses. Remarkable progress has been made in reducing the transmission loss from 20 dB/km to about 0.2 dB/km, and in the recent years this has further reduced to 0.002 dB/km [23].

The attenuation can be classified into two:

- i) Intrinsic losses – this refers to losses caused by substances inherently present in the fibre like impurities and imperfections in the glass. An example of an intrinsic loss is material absorption and Rayleigh scattering.
- ii) Extrinsic losses- this defines losses or attenuation caused by external forces such as macrobending.

The loss mechanisms contributing to attenuation in an optical fibre are;

- a) Absorption,
- b) Scattering due to inhomogenities in the core refractive index (Rayleigh scattering),
- c) Scattering due to irregularities at the boundary between core and cladding,
- d) Bending loss (macro and micro bending),
- e) Loss at joints and connectors,
- f) Coupling losses at the input or output and mode coupling and leaky modes losses.

The major loss mechanisms are discussed in the following sections.

2.6.1 Material Absorption

Absorption occurs as a result of imperfections and impurities in the fibre and can be defined as the portion of attenuation resulting from the conversion of optical power into other forms of energy, such as heat. The traces of hydroxyl radicals and transition metals contribute extensively to absorption in optic fibres. Absorption accounts for 3-5 % attenuation and the absorbed light is converted to vibration energy. Great care at the manufacturing stage can significantly reduce losses due to absorption. Fundamental absorption due to hydroxyl ions is present at $\lambda = 2730$ nm. The harmonics or overtones of fundamental absorption occur at wavelengths $\lambda = 950$ nm and 1380 nm, as shown in Figure 2.5. The absorption due to hydroxyl ions arises from the basic stretching vibration of the O-H bond [21, 22].

Transition metal ions (for example Fe^{++} , Cu^{++} , Cr^{++}) introduced into fibres during fabrication produces a loss due to absorption at wavelengths greater than 800 nm but this is negligible in ultra low loss fibres which can attributed to their composition. Acceptable levels require that concentrations of transition-metal ions be kept below about 1 part in 10^9 so that its contribution to attenuation is kept below 1dB/km at $\lambda = 1\mu\text{m}$ and that of OH^- radical concentration should not exceed 1 part in 10^7 . There is a tail of infrared absorption by SiO-coupling present at wavelengths around 1400 nm – 1600 nm. The interaction between the vibrating bond of (Si-O) and the electromagnetic field of the optical signal causes intrinsic absorption as light energy is transferred from electromagnetic field to the bond. Intrinsic absorption is also present in the UV region caused by electronic absorption bands resulting in electron transition present at around the wavelength 800nm producing a loss of about 0.3 dB/km [21, 22].

2.6.2 Scattering

Scattering is present in the following forms; Rayleigh scattering, Mie scattering, Raman and Brillouin. Raman and Brillouin have little effect on transmission whilst Rayleigh is the most predominant of all the forms of scattering. The local microscopic variations in composition of glass produced in the guide during glass melting and fibre drawing gives rise to spatial fluctuations of the refractive index. These variations are small compared to optic wavelength and will cause light to be scattered, the scattering known as Rayleigh scattering. It has been observed that the scattering is proportional to $1/\lambda^4$ and also has an angular dependence proportional to $(1 + \cos^2 \theta)$, where θ is the angle at which the scattered light strikes the core/cladding interface. Rayleigh scattering becomes rapidly smaller at longer wavelengths since it is proportional to λ^{-4} [22].

The loss caused by this mechanism can be minimized by cooling the melt from which the fibre is drawn in as carefully controlled a manner as possible [3]. Given the nature of how Rayleigh scattering arises, it is likely to be higher in multi component glasses because of compositional variations. Rayleigh scattering produces a maximum loss in the ultraviolet region, and in the wavelength around 800 nm to 1000 nm, giving a loss of about 0.6 dB/km [22].

When the inhomogenities in the glass structure are comparable in size to the guided wavelength, Mie scattering is observed, though it is insignificant in commercial fibres. This is mainly forward scattering and cannot be easily separated from that due to tunnelling out of

the highest order modes propagated in the fibre under the conditions in which scattering is usually measured. Large imperfections whose size is greater than the wavelength exhibit a wavelength independent scattering that has a quite random angular dependence. The fibre drawing peak reported by Kaiser or absorption shown by the fibre is accompanied by a resonance scatter easily distinguished by its wavelength correspondence with the associated absorption mechanism.

2.6.3 Mode coupling and leaky modes

Mode coupling refers to the transfer of power from one mode to another as light propagates in a fibre and it is influenced by variations in core diameter and core/cladding refractive index difference along the length of the fibre. This has an overall effect of reducing the signal power as this power is also transferred to the radiation field. According to the study done by Marcusse for any two modes with propagation constants β_x and β_y there will be a coupling parameter

$$\theta_{xy} = \beta_x - \beta_y , \quad 2.32$$

which will be particularly effective in inducing coupling. Some rays at the input of the optic fibre may not be captured by the core but instead will escape into the cladding where they will propagate a significant distance before dying out. These constitute leaky modes or cladding modes and can couple with the higher order modes of the core resulting in increased loss of the core power. Leaky modes can be suppressed by placing a high-loss material

outside the cladding surface or a material whose refractive index matches that of the cladding.

2.6.4 Bending Loss

Bending loss in the form of macro and microbending is another loss mechanism that contributes to loss as light propagates along the fibre. Microbend loss is due to microscopic fibre deformations in the core-cladding interface and is usually caused by poor cable design and fabrication [7]. Non- uniform lateral stresses during the cabling and the deployment of the fibre in the ground introduces microbends [5]. Macrobends are bends on a fibre having a large radius of curvature (bend)/ diameter relative to the fibre core diameter that is $R \gg a$ where a , denotes the core radius, and R the radius of curvature [5, 6]. Macrobend losses are usually encountered during the in-house and installation process of the optic fibre.

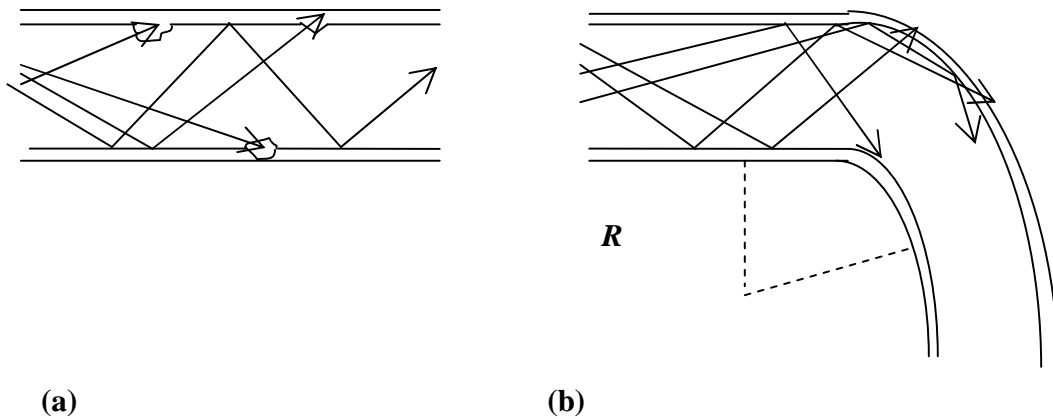


Fig 2.6: (a) Microbending; (b) Macrobending

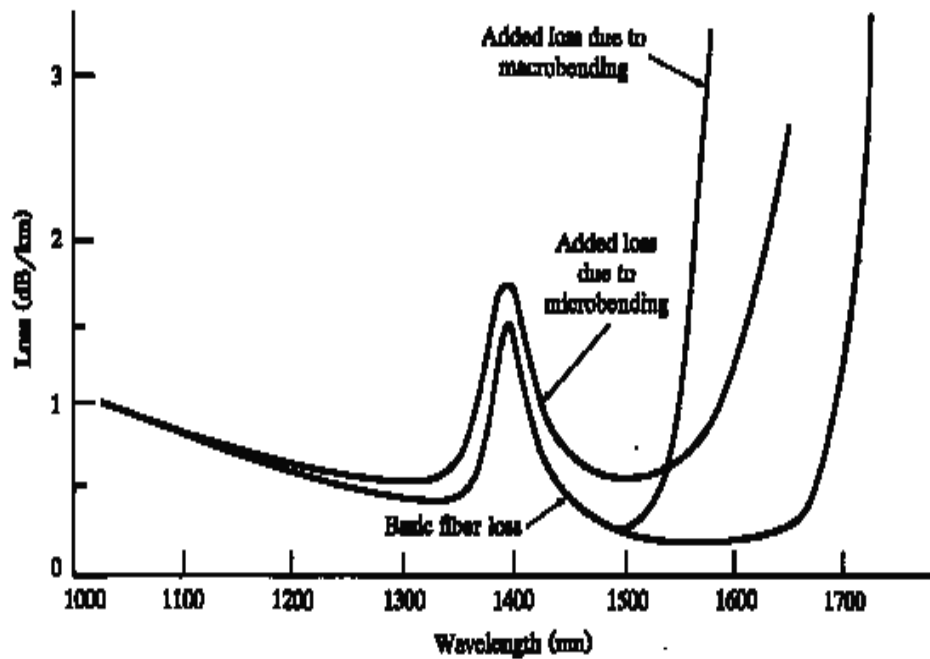


Fig 2.7: Loss due to microbending and macrobending on basic fibre power loss

Figure 2.7 further illustrates the extra loss introduced due to micro and macrobending in an optic fibre.

2.6.4.1 Microbending

Microbends are microscopic bends of an optic fibre that arise due to poor cable design and transportation. Gloge and Marcuse have shown that such bends do not need to be of large amplitude to cause losses of a few dB/km [23, 24]. It is therefore important that care should be taken in order to minimise these perturbations that may have an effect on the fibre's transmission. The small bends change the angle at which light hits the interface and if that occurs at an angle smaller than the critical angle, light will be refracted into the cladding leaking out instead of being reflected within the fibre. Microbending loss can be investigated by winding fibres under constant tension onto a drum surface that is not perfectly smooth.

The tension forces the fibres to conform to the slight surface irregularities, which can result in an increase in the optical loss in the order of 100 dB/km as a result of the microbends [25].

2.6.4.2 Macrobending

Macrobends can be characterized by a bend angle, bend diameter or a bend radius also known as radius of curvature. When a fibre is bent the incident angle is compromised and total internal reflection fails and thus the light is no longer confined and guided by the core of the fibre. This is known as the ray diagram approach of viewing macrobending. The overall effect is that the signal is attenuated as a result of this loss [7]. Macrobending can also be analysed using the mode field approach where a wave front perpendicular to the direction of travel must be maintained. It follows that at sharp bends, the outer part of the mode field must travel faster than the inner part to maintain this wave front. This would mean the outer part propagating at a velocity more than the velocity of light which is impossible and we therefore have the energy of this outer part dissipating into the cladding as heat.

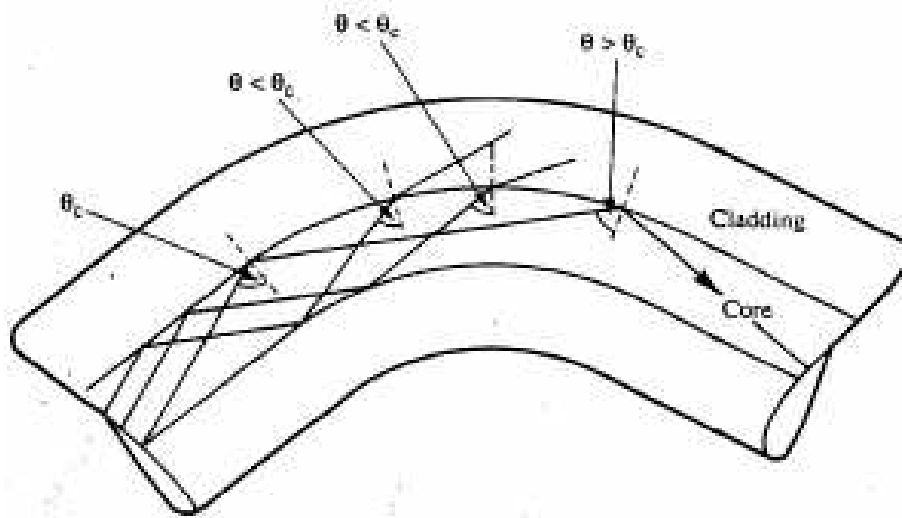


Fig 2.8: Ray field diagram approach

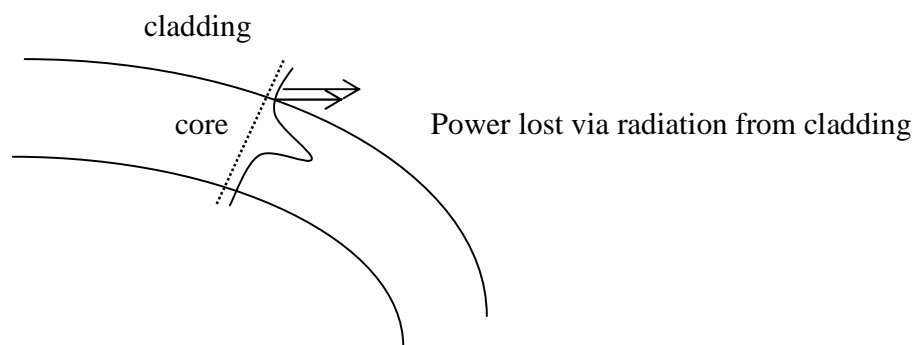


Fig 2.9: Mode field approach

A number of scientists have researched and made findings on macrobend losses in both single and multimode optic fibres [6, 7, 9, 23, 26]. Macrobend losses have been found to depend on the bend diameter/radius of curvature of the optical fibre and the wavelength of the propagating light in the case of SMF. If radius of curvature of the bend of the optical

fibre is small and the transmitted light is long, the macrobending loss in the optical fibre has been observed to increase.

It has been observed that below a critical radius, the bend radius beyond which attenuation rapidly increases, the macrobending loss becomes significant and noticeable [7, 27]. It is therefore crucial to avoid radius of curvatures approaching the critical radius in installations and transportation of these optic fibre cables. Findings by Quino, suggests that loss due to bending in the visible light range is more pronounced than loss due to other loss mechanisms such as absorption [26].

Multimode fibres measurements are a bit difficult to do in that light travels in several modes and the effect of macrobending can be insignificant such that it may be difficult to detect in an experimental situation. These modes have their own bend sensitivity and it is difficult to measure modes loss independently. Researches on macrobending loss in multimode fibres have made use of models [8, 9]. Kauffman et al [9] have shown that the overall power loss that is due to bending has a non monotone structure as a function of the radius of curvature of the bending. Derivation of a loss coefficient associated with the curvature loss is done for a whole fibre, but to do so require knowledge of both the initial power distribution among the modes and the coupling between the modes which is assumed negligible. The bend-loss model has been used to determine macrobend losses as a function of the number of mandrel wraps (turns) and the launch conditions.

The number of modes propagating in the multimode fibre is dependent on the bending diameter. At a small radius of curvature new modes are added rapidly and slowly for an increasing radius of curvature. Computations and measurements have shown that the

multimode nature of MMF makes their bend loss behaviour significantly different from that of SMF because only the highest order are bending sensitive that is those closer to the cladding. The bending loss was also found to depend strongly on the launch conditions [8].

2.7 Light Source

The ideal source should emit light continuously and appropriate care should be taken in component selection for the design of the light source circuit. Several light sources can be used from LEDs, laser and mercury vapour lamp. In actual operation, because of their properties single mode fibres make use of laser as the signal source whilst multimode fibres use LEDs. However for research purposes mercury vapour lamps, LEDs and lasers are used interchangeably in order to investigate wavelength dependence on fibre losses.

When using LEDs an astable multi vibrator pulses can be used to drive the LED. This is based on the fact that an astable multi vibrator has no stable state but keeps changing between two unstable states. In this case it will be switching between on and off state of the LED, and if components are carefully chosen, the off state time can be reduced so that to the eye the LED will be seemingly on all the time.

2.7.1 Astable Multivibrator

The 555 timer is an integrated circuit that can be used as an astable multivibrator. The output of the multivibrator is used to power the LED through a low value resistor. The 555 can introduce some noise into the circuit and therefore a low noise 555 must be used.

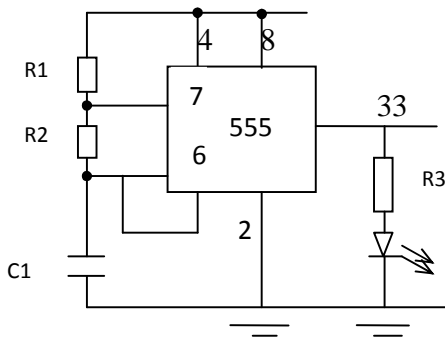


Fig 2.10: 555 timer connected for astable operation

The output is in the high (ON) state for a time t_H ,

$$t_H = 0.693(R_1 + R_2)C \quad 2.32$$

And output is in the low (OFF) state for a time t_L ,

$$t_L = 0.693R_2C \quad 2.33$$

The period of the output waveform is a sum of the two,

$$T = t_L + t_H = 0.693(R_1 + 2R_2)C \quad 2.34$$

From which the frequency of the 555 timer for the astable operation is obtained as

$$f = \frac{1}{T} = \frac{1.44}{(R_1 + 2R_2)C} \quad 2.35$$

The duty cycle developed by such a circuit is then given by:

$$\text{Duty cycle} = \frac{t_H}{T} = \frac{t_H}{t_L + t_H} = \frac{R_1 + R_2}{R_1 + 2R_2} \quad 2.36$$

2.8 Light Detector

A light detector circuit can be used in place of an optical spectrum analyser to measure light intensity in order to determine the attenuation in optic fibres. Photoelectric devices for example photodiodes, phototransistors and light dependent resistors (LDR) can be used to built the detector circuit. The choice of photoelectric device in any design depends on the sensitivity and stability of the detector under the operational conditions as well as a reasonable range of values for a known change in intensity.

2.8.1 LDR light detector circuit

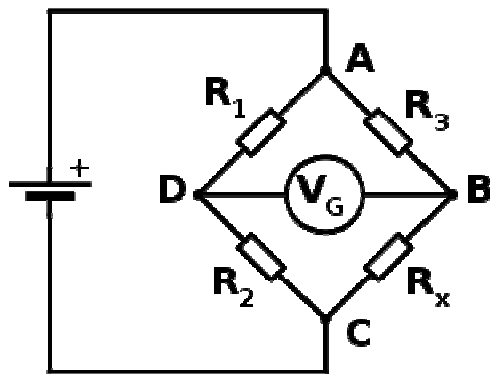


Fig 2.11: LDR light detector circuit

In this configuration the out of balance voltage V_G is measured. The resistance, R_x (LDR) proportional to the light intensity is then calculated using equation 2.39.

2.8.2 Wheatstone bridge theory

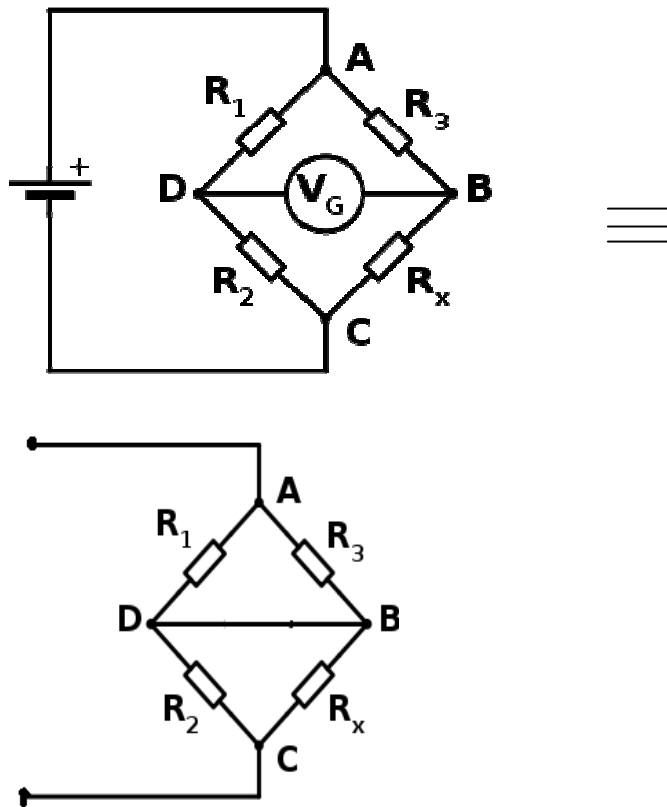


Fig 2.12: Wheatstone bridge connection and its equivalent circuit

Solving the bridge equations assuming balance conditions voltage V_G can be calculated where from first principles, $I_3 = I_x$ and $I_1 = I_2$. The desired value of R_x at balance condition is then:

$$R_x = \frac{R_2 R_3}{R_1} \quad 2.37$$

Knowing all the four resistor values and the supply voltage (V_S), and having the resistance of the galvanometer high enough so that I_g is negligible, the voltage across the bridge (V_G) can

be found by working out the voltage from each potential divider and subtracting one from the other to get,

$$V_G = \frac{R_x}{R_3 + R_x} V_s - \frac{R_2}{R_1 + R_2} V_s \quad 2.38$$

where V_G is the voltage of node B relative to node D.

In the case where measurements are done at out of balance position of the bridge, the measured value of V_G can then be used to calculate value of corresponding R_x . Substituting all the known values of R_1 , R_2 , R_3 Vs and at a particular V_G , R_x is given by,

$$R_x = \frac{R_3 (V_G + V_s) \left(\frac{R_2}{R_1 + R_2} \right)}{V_s - (V_G + V_s) \left(\frac{R_2}{R_1 + R_2} \right)} \quad 2.39$$

2.8.3 LDR Theory

The resistance of the LDR varies according to the amount of light that falls on it. The resistance decreases with increased light intensity, that is it has a negative co-efficient. For a typical LDR the relationship is given by [29]:

$$R_x = \frac{500}{Lux} K\Omega \quad 2.40$$

$$\text{So that } Lux = \frac{500}{R_x} \quad 2.41$$

CHAPTER THREE: MATERIALS AND METHODS

3.1 Introduction

Materials used in carrying out the research are listed in this chapter. The chapter also describes designs made, measurements taken and precautions observed in taking measurements and making designs.

3.2 Materials

3.2.1 Light Source

The following materials were used to construct a light source;

- 5 mm extra illuminant LEDs (green) wavelength 520 – 560 nm
- NE55532P 555 timer
- 250K Ω variable resistor
- Resistor 1
- 12V Power supply
- Resistor 2
- Aluminium box painted blank inside and outside with a 2.1mm slit

3.2.2 Light Detector

- 12 V digital power supply
- UNIT-T UT39A Digital multimeter
- Resistors $R_1 = 100\text{ K}\Omega$, $R_2 = 100\text{ K}\Omega$, $R_3 = 12\text{ K}\Omega$
- 26.6 cm \times 16 cm \times 19 cm wooden box
- Vero board
- LDR (Light Dependant Resistor)

3.2.3 Fibre and bending material

- 1 \times 2 m Single Mode fibre
- 1 \times 2 m Multimode fibre
- Musking tape
- Metre rule
- 3 x clamp and stand
- Hollow cylinders of several diameters

3.2.4 Additional materials

- 2 x Adjustable stands
- Optical bench
- 2 x biconvex lenses
- Aluminium box painted blank inside and outside with a 2.1mm slit

3.3 Method

3.3.1 Construction of a light source circuit

The light source circuit was to serve as the signal source. The circuit was connected as in Figure 2.10. The circuit was fine tuned by adjusting the variable resistor in order to get the LED at its brightest point. The light source was enclosed in black aluminium box with 2.1mm slit. The box ensured the LED was isolated from external light sources in the lab. Using an oscilloscope the period, frequency and duty cycle of the circuit were determined. The light coming out of the slit was then focused into tiny beam spot by two lenses.

3.3.2 Construction of light detector circuit

Two circuits were initially designed for light detection;

- i) Using a phototransistor
- ii) Using an LDR

3.3.2.1 Phototransistor Light detector circuit

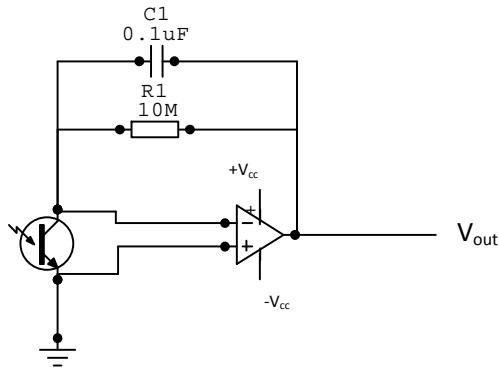


Fig 3.1: Phototransistor light detector circuit

The circuit was connected as shown in figure 3.1. The response graphs of the two available different phototransistors were determined in turn by varying the light intensity falling on the phototransistors. See figure 4.1 and 4.2.

3.3.2.2 LDR light detector circuit

The circuit was connected as shown in figure 3.2. The response graph of the circuit in figure 3.2 was determined by varying the light intensity falling on the LDR. The response graph of the LDR is shown in figure 4.3.

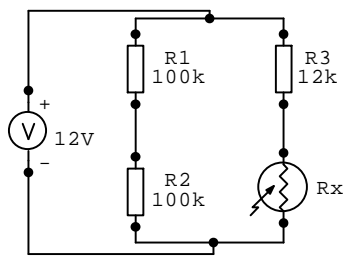


Fig 3.2: Light Detector Circuit

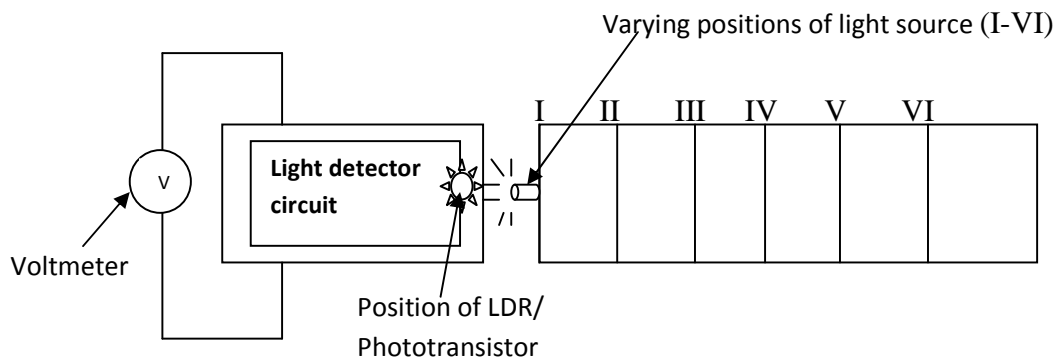


Fig 3.3: Connection for determining response curve for the two different designs

The response graphs for LDR and the two different phototransistors were compared from which the LDR light detector circuit was adopted for use as the detector. This was because it was more stable, sensitive and it also gave a wide range of values over the varying intensities.

The current voltage (IV) characteristics of the LDR light detector were then established using the connection in figure 3.4. The respective components were soldered onto a Vero board and the circuit enclosed in a wooden box. The wooden box was painted black inside to isolate the

light from the optic fibre end and had terminals to which bias voltage and the digital multimeter were connected.

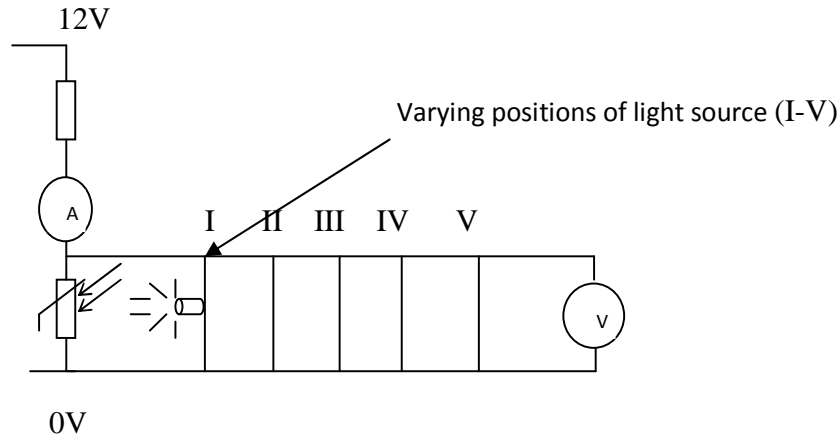


Fig 3.4: Circuit for determining I-V characteristics of an LDR

3.3.3 Measurements

3.3.3.1 Measurements with Single Mode Fibre

The single mode fibre was carefully aligned to the light (green) coming out from the aluminium box slit and positioned at the focal point of one of the lens in order to maximise the light intensity getting into optic fibre. The output from the optic fibre was focused onto the LDR and the out of balance voltage of the bridge recorded. Measurements were done for both the straight and bend conditions of the fibre.

To bend the fibre hollow cylinders of varying diameters were used and the same procedure was repeated using red and blue LEDs. The bend diameters used were 10.02cm, 7.41cm, 6.50cm, 5.11cm, 4.19cm, 3.33cm, 2.82cm, 2.15cm, and 1.92cm. The bend diameters were

measured using a Vernier calliper's on various positions across the lengths of the cylinders for precision and accuracy reasons.

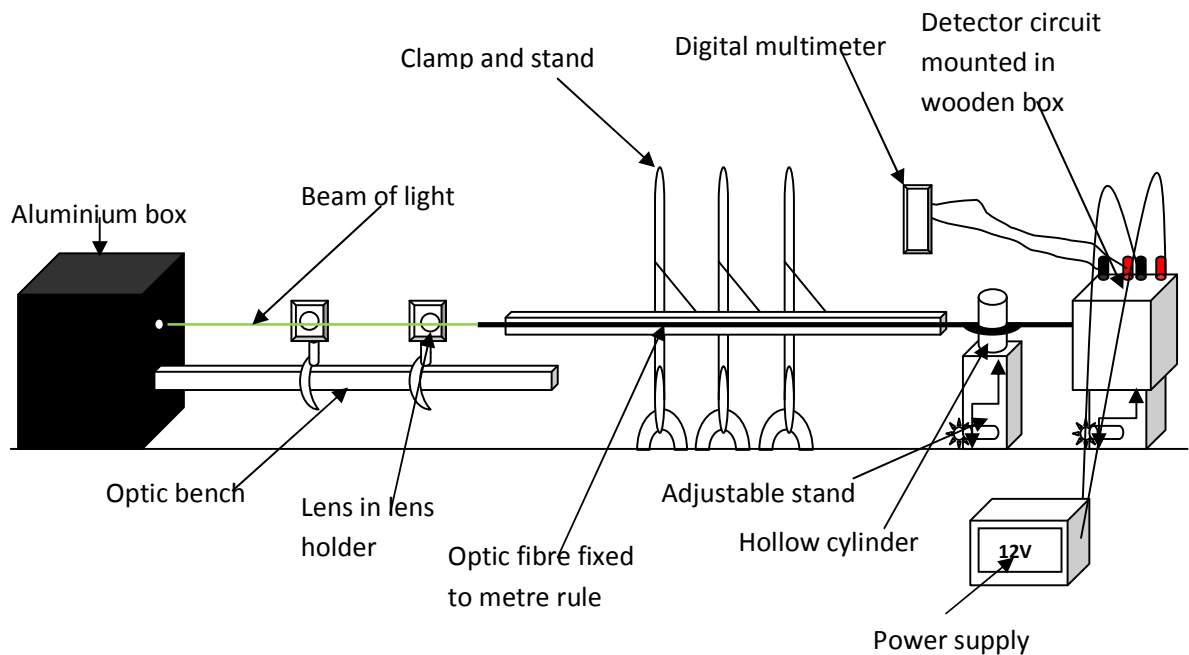


Fig 3.5: Schematic diagram of the experimental set up

3.3.3.2 Measurements with Multimode fibre

The same procedure was repeated using the Multimode fibre in place of the single mode fibre.

3.4 Precautions

- Light source was enclosed in a black aluminium box to isolate the LED from other external sources of light. A slit was also used to narrow /collimate the beam.

- b) The optic fibre was maintained horizontal during the experiment so that bending losses would be limited to bending achieved using the hollow cylinders.
- c) The light detector circuit was mounted in a black wooden box to isolate it from other light sources to ensure that whatever reading generated on the light detector, was due to light exclusively from the optic fibre.

3.5 Sources of Errors

- a) Optical measurements are unstable, and changes could be noticed when there were disturbances/movement on the experimental surfaces (tables).
- b) Besides the value of resistance of the LDR being light dependant it is also temperature dependant and during the period of the experiment sudden changes in temperature caused fluctuation in readings.
- c) Ideally the experiment should have been performed at the optimum operating wavelengths of the fibres which is 1310 nm and 1550 nm for SMF and 850 nm and 1300 nm for MMF ; however an improvisation using a green LED (wavelength about 520-565 nm) was done due to resource constraints.
- d) Coupling efficiency – the coupling efficiency of light to the optic fibre was compromised as lenses secured in lens holders had to be used. Also the size of the focused spot was bigger than the numerical apertures for both of the fibres.
- e) The responsivity of the light detector was dependant on the direction of the incident light and so when this changed it would mean a change in the experimental conditions that was meant to remain constant throughout the experiment.

- f) Calibration of the light detector – there was no standard to which the light detector could be calibrated against, instead all measurements are relative.

CHAPTER FOUR: RESULTS AND DISCUSSION

4.1 Introduction

The chapter presents results of all the measurements taken including those for construction of the light detector and its characterisation. Measurement results for the experiment with single and multimode fibres are also presented and discussed in detail.

4.2 Phototransistor Response

The phototransistors response curves are shown in Figure 4.1 and Figure 4.2

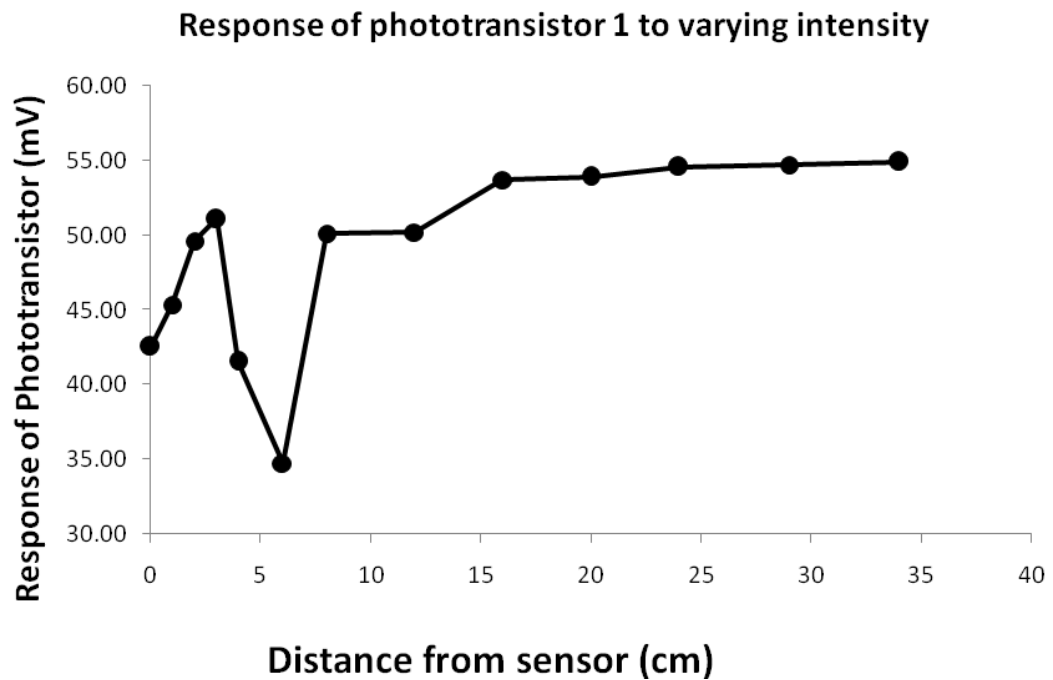


Fig 4.1: Response of Phototransistor 1 to varying light intensity

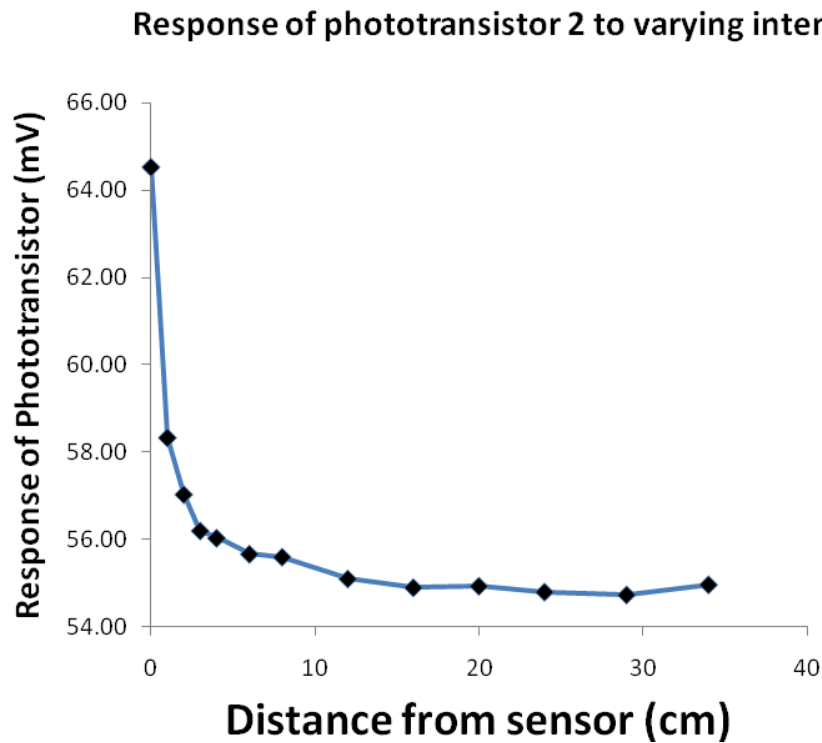


Fig 4.2: Response of phototransistor 2 to varying light intensity.

The two phototransistors show little variation to the varying light intensity with an average response range of 42-65 mV. Significant response of light detector is noticed when the light source is only a few centimetres from the photoelectric device. The behaviour of phototransistor 1 cannot be accounted for based on theory of operation and the dip at data point corresponding to distance 6 cm from phototransistor occurred even after repeating the experiment several times. The unusual fluctuations could be as a result of an unstable gain given the fact that the photoelectric device was an active leg and contributed to R_f a

determining value for the gain of the circuit. This would not serve the purpose of the experiment as it involved sensing minute changes in light intensity.

4.3 LDR Characterisation

4.3.1 LDR Response

Figure 4.3 is a response graph for the LDR to varying light intensity.

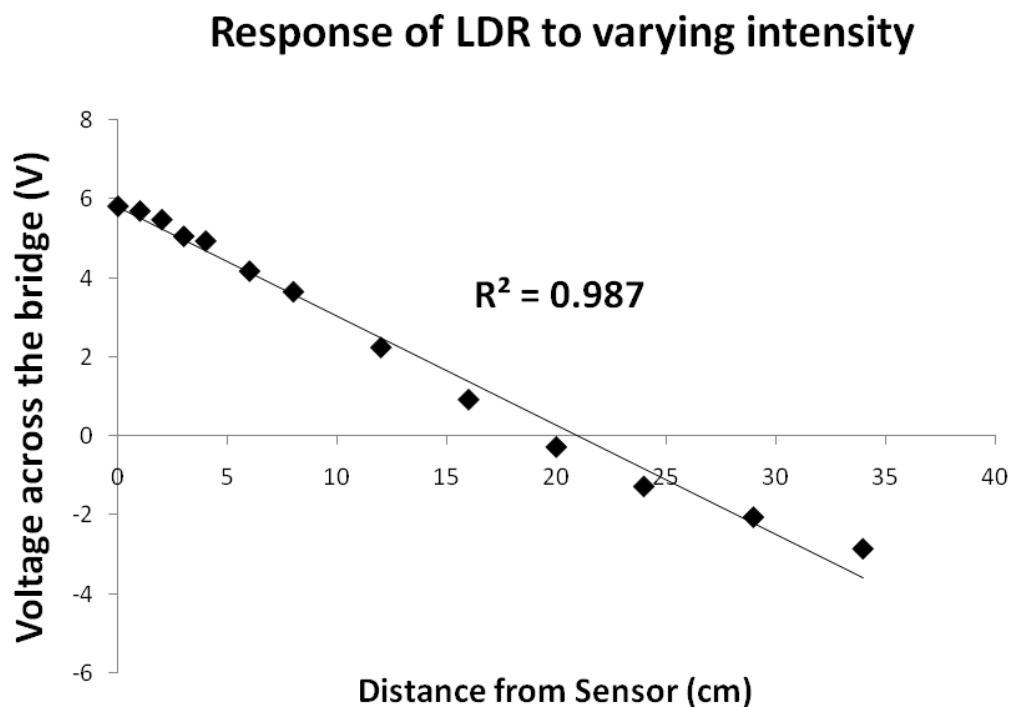


Fig 4.3: Response graph for the LDR

The LDR showed a linear variation with intensity swinging from negative to positive voltage.

The readings were spread over a wider range compared to that of the detector circuit using

phototransistors with values ranging from -2 to 6V. The light detector using LDR was therefore adopted for use as the light detector in this experiment.

4.3.2 Current Voltage characteristics of LDR

The current voltage characteristics of the LDR are shown in Figure 4.4.

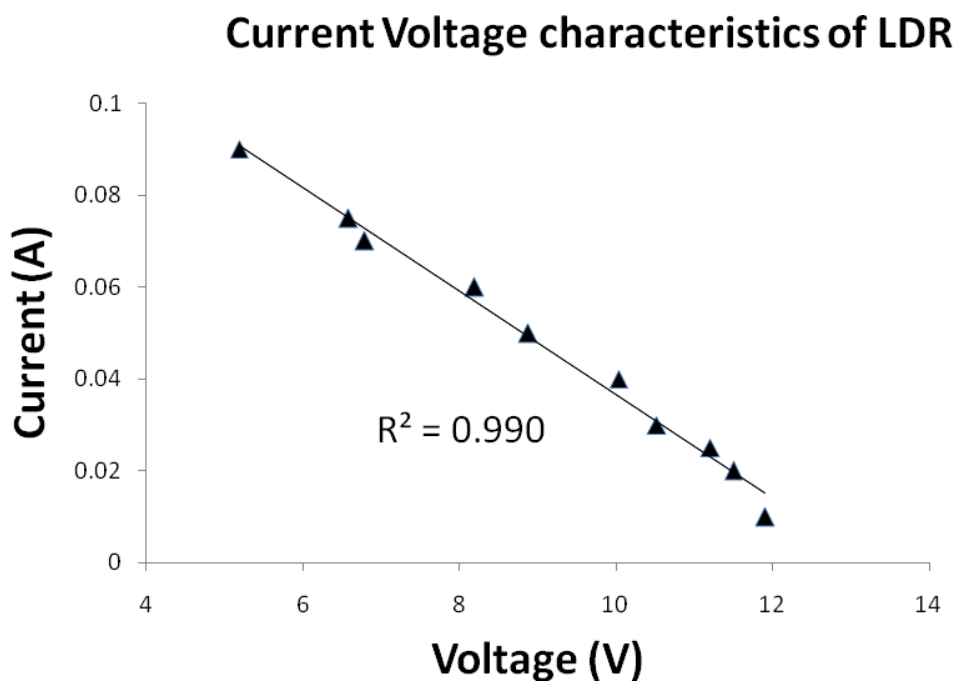


Fig 4.4: LDR current voltage characteristics

There is a direct linear relationship between the voltage and current flowing through the LDR for the varying intensity values. This verifies Ohm's law which states that the electric current (I) flowing through a conductor is directly proportional to the potential difference (V) between its ends, that is $V = IR$.

4.4 Measurements with Single Mode Fibre

Measurements were done for both straight and bend conditions of the fibre. Results are shown in Table 4.1.

Table 4.1: Single Mode Fibre Measurement Results

Bend Diameter (cm)	Vg (V)	R_x (Ω)	Intensity(Lux)
0.00	4.63	92727.3	5.39
10.02	4.90	118909.1	4.20
7.41	4.95	125142.9	4.00
6.50	5.03	136837.2	3.65
5.11	5.13	153517.2	3.26
4.19	5.19	166328.2	3.01
3.33	5.26	182594.6	2.74
2.82	5.33	202925.4	2.46
2.15	5.43	238434.8	2.10
1.92	5.62	369457.0	1.35

Bend diameter = 0.00cm corresponds to measurement when fibre was straight. R_x was calculated using equation 2.39, where $R_3 = 12 \text{ k}\Omega$, $V_s = 12\text{V}$ and $\frac{R_2}{R_1 + R_2} = 0.5 \text{ } \Omega$. The illuminance or light intensity in Lux was determined using the relationship as in equation 2.41.

4.4.1 Calculation of Attenuation

$$\text{Attenuation (dB/km)} = \frac{-10}{L} \log \left(\frac{I_o}{I_i} \right)$$

A negative sign was factored in for calculations in order to take into account the fact that attenuation is a loss and therefore is negative. Intensity was also assumed in place of power, this is because light intensity is a measure of power received per unit area, and since attenuation is a ratio output power to the input power, the unit areas would eventually cancel. This makes the calculated values for attenuation relative and hence the values might not reflect the actual attenuation in the optic fibres but allow for comparison of power loss in the two optic fibres.

Table 4.2: Attenuation in a single mode fibre

Bend Diameter (cm)	Input Intensity (lux)	Output Intensity (lux)	Attenuation (dB/km)
0.00	8.26	5.39	926.09
10.02		4.20	1466.13
7.41		4.00	1577.08
6.50		3.65	1771.07
5.11		3.26	2020.84
4.19		3.01	2194.88
3.33		2.74	2397.49
2.82		2.46	2626.73
2.15		2.10	2976.90
1.92		1.35	3927.87

The attenuation figure for the Single mode fibre when it was straight = 926 dB/km. The attenuation value is very big compared to other values obtained for example, $2.26 \times 10^{-2} \text{ dB/m}$ which translates to 22.6 dB/km for wavelength range 366-578 nm

mercury vapour lamp light [6]. The extremely high value of attenuation can be accounted for by the low coupling efficiency of light into the optic fibre. Points of measurement of input power into the optic fibre could not be precisely determined and this could have contributed in a higher value of input intensity than the actual intensity getting into the fibre.

4.5 Measurements with Multimode Fibre

Measurement results of the multimode fibre for both the bend and straight conditions are shown in Table 4.3

Table 4.3: Multimode Fibre Measurement Results

Bend Diameter (cm)	V_g (V)	R_x (Ω)	Intensity(Lux)
0.00	5.96	3376235.29	0.15
10.02	5.97	4102285.71	0.12
7.41	5.97	4788000.00	0.10
6.50	5.97	5224363.64	0.10
5.11	5.97	4788000.00	0.10
4.19	5.98	5748000.00	0.09
3.33	5.98	5748000.00	0.09
2.82	5.97	5224363.64	0.10
2.15	5.98	7188000.00	0.07
1.92	5.98	6388000.00	0.08
Input Value	4.015	60544.08	8.26

There was little variation in the measured V_g values for the multimode case even when macrobending was introduced and this indicates minimum changes in the total signal loss in the optic fibre due to macrobending for the multimode fibre.

4.5.1 Calculation of Attenuation in Multimode Fibre

Same procedure was followed as was done for the single mode fibre and results are shown in table 4.4.

Table 4.4: Attenuation in a Multimode fibre

Bend Diameter (cm)	Input Intensity (lux)	Output Intensity (lux)	Attenuation (dB/km)
0.00	8.26	0.15	8732.21
10.02		0.12	9155.18
7.41		0.10	9490.82
6.50		0.10	9680.22
5.11		0.10	9490.82
4.19		0.09	9887.63
3.33		0.09	9887.63
2.82		0.10	9680.22
2.15		0.07	10373.09
1.92		0.08	10116.87

Attenuation values for the multimode fibre are extremely high, where for straight condition of the fibre, attenuation = 8732.21 dB/km for the multimode that is approximately 10 times the value for single mode fibre. However there was little variation in the attenuation coefficient with change in bending diameter.

For the single mode case, the power loss due to macrobending increases exponentially as the bend diameter increases as seen by the almost linear graph of $\ln \alpha$ (attenuation) versus the bend diameter Figure 4.5 with an R^2 value = 0.857. No significant trend can however be specified for the multimode, Figure 4.6 show a close to constant variation of attenuation with bend diameter with the values for $\ln \alpha$ oscillating between 9.14 and 9.20 dB/km.

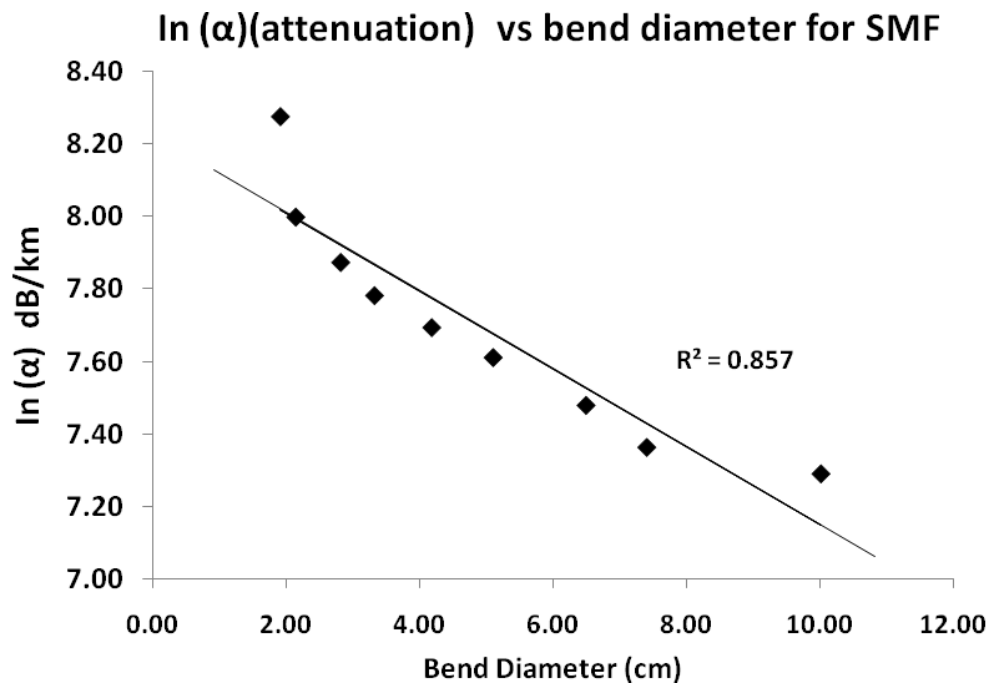


Fig 4.5: In (α)(attenuation) vs bend diameter for SMF

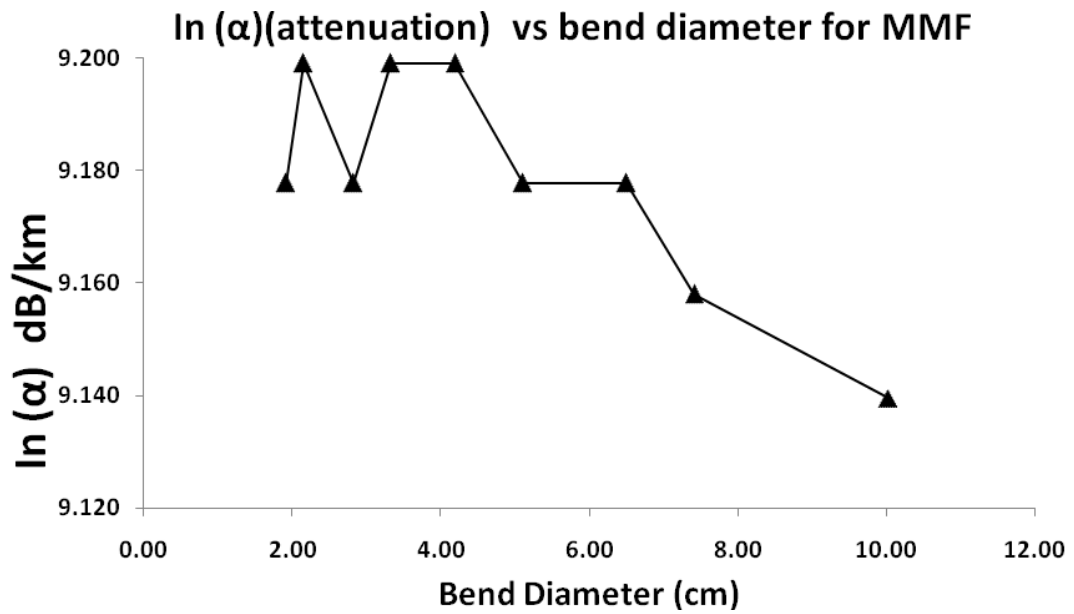


Fig 4.6: In (α)(attenuation) vs bend diameter for MMF

Trends of attenuation in SMF and MMF

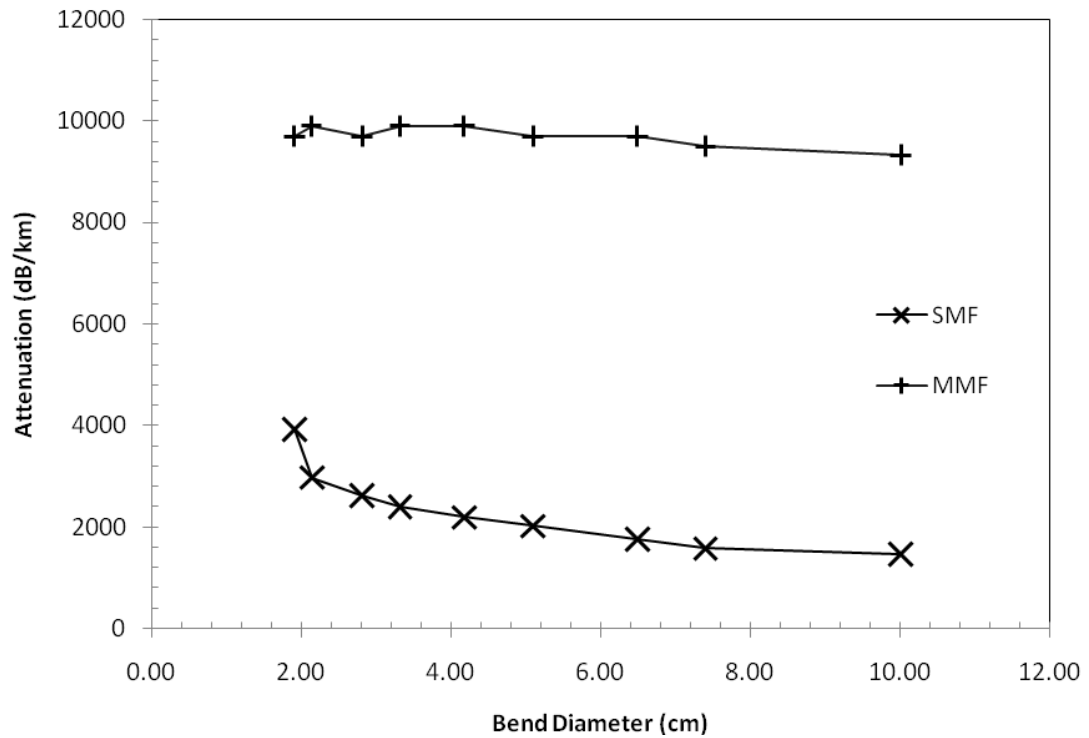


Fig 4.7: Comparison of Macrobend losses in SMF and MMF

From Figure 4.7 it can be deduced that attenuation is more pronounced in multimode fibres than it is single mode fibres. Characteristic values of attenuation for the optic fibre for example for bend diameter 10.02cm are 1466.13 dB/km for single mode compared to 9316.56 dB/km for multimode fibre. This is in agreement with theory where in single mode fibre, because of the small core and single light wave (mode) any distortion that could arise from overlapping modes is eliminated and hence the single mode provides the least signal attenuation [3]. Extra transmission loss is introduced in multimode fibres due to their nature where light propagates in several modes. The various modes of light introduce modal dispersion where the different modes of light arrive at the receiving end of

the fibre at different times causing a spreading effect. There is also mode coupling and leaky modes being more prevalent in multimode fibre contributing to further attenuation described in section 2.6.3.

The power loss as a consequence of macrobending is extremely low in the MMF and was difficult to quantify experimentally. Kauffman et al highlight the same effect and instead assume a simple hypothesis about the distribution of power among the modes where obtained results are used to analyse the trend of the overall loss of the multimode fibre with the radius of curvature [9]. The general trend for the SMF was such that the attenuation increased with decrease in the bending diameter. For larger bend diameters the attenuation was tending to become constant suggesting the contribution of attenuation to the overall attenuation at this point was therefore minimum. The major contributors of attenuation for larger and larger bend diameters would be absorption, scattering and other loss mechanisms. The result conforms to findings by other authors [6, 9, 26, 28]. The wavelength used in this experiment also contributed to more attenuation in the optic fibres as it is not the optimum wavelength for either of the fibres.

CHAPTER FIVE: CONCLUSION AND RECOMMENDATIONS

5.1 Introduction

The chapter sums up the findings of this research. Success of the research according to the laid out objectives is discussed as well as recommendations for future work along the lines of this research.

5.2 Conclusion

The research sought to investigate and compare the attenuation in Single Mode Fibre (SMF) and Multimode Fibre (MMF) due to macrobending. In order to do so improvisations were done for the light source using 555 timer astable multivibrator powering a green LED and an LDR in a Wheatstone bridge circuit that served as a light detector and optic fibres off-cuts used for the carrying out of the experiment.

When there was no macrobending in both of the fibres attenuation was recorded, attenuation associated with scattering and absorption and other loss mechanisms. Overallly signal power loss was higher in MMF than in SMF as seen in Figure 4.7 and this explains the reason why single mode fibre are usually preferred for long distance transmission. The loss in SMF without macrobending was found to be 926 dB/km and that for MMF to be 8732.21 dB/km.

Attenuation in the SMF increases as the bend diameter decreases and does so in an exponential manner. It is a different case for the MMF, where the attenuation trend seemed not existant and was difficult to quantify. However from the results it can be deduced that single mode fibres are more susceptible to macrobending than multimode fibres. For instance the single mode has an attenuation

due to macrobending only for bending diameter 4.19 cm equal to 1268 dB/km while the multimode fibre has an attenuation due to macrobending only equal to 1155 dB/km.

The results confirm that macrobending has a significant contribution to the overall attenuation in an optic fibre particularly in the SMF, hence it is important that macrobending be considered and characterised for efficient signal transmission without compromise to quality.

Precautions were observed in order to minimise inconsistencies in the carrying out of the experiment and improve in the accuracy of the results. Some errors could not be completely eliminated, these such as given in section 3.5. More accurate determination of attenuation in the optic fibres in this research could be achieved by using a more standard and sensitive optical meter for example an OTDR or Optical spectral Analyser. Further improvements would also include use of a proper optical bench using the specified operational light sources for the optic fibres that is LED for multimode fibre and laser for single mode fibre.

5.3 Recommendations

For further work it is recommended that the same work be done at operational wavelengths of the optic fibres using the ideal light sources for each of the fibres. Comparison would be easier if say this is done at wavelength 1310 nm/1300 nm common and almost equal for both of the optical fibres. It would also be of great importance if the bend diameter could be lowered a bit more so as to ascertain how much more the fibres can bend before reaching the critical radius (diameter) that is the radius (diameter) beyond which the attenuation will rapidly increase.

Of interest would be also investigating and characterising the macrobending attenuation trend for the recently introduced, the Plastic optic fibre (POF). The combination of this with other factors like cost, transmission speed and bandwidth would enable selection of any of these three for use such as to minimise cost yet not compromising on signal quality and strength which is the main thrust of the telecommunication industry.

REFERENCES

- [1] H. J. R. Dutton, Understanding Optical Communications (International Technical Support Organisation), 1998.
- [2] N. Massa, Fundamentals of Photonics (Fiber Optic Telecommunication), 2000.
- [3] K. Munjeri, Fibre Optic Lecture Notes, Department of Physics, University of Zimbabwe, 2010.
- [4] Optical Fiber Tutorial , <<http://www.fiberoptics4sale.com/Merchant2/optical-fiber.php>>, (2011, October 5). Optic Fiber - Communication Fiber.
- [5] K. Witcher, Fiber Optics and Its Security Vulnerabilities, University MARY Washington, 2005.
- [6] G. Getu, Experimental Technique to Characterize Macrobending Loss in Single Mode Fiber, Addis Ababa University, 2010.
- [7] Macrobending Attenuation in a single mode Optic Fiber, (2003), <<http://www.redandwhite.ws/hexagon/EE/Exemplary%20Extended%20Examples/Ashbury%20Physics%20201.pdf>>, (2011, September 26). International Baccalaureate Extended Essay.
- [8] D. Molin, P. Matthijsse, G. Kuyt and P. Sillard, Reduced Bend Sensitivity of Multimode Fibers in Fttx applications, Draka Comteq France, Marcousis, France.
- [9] K.S. Kaufman, R. Terras and R.F. Matthis, Curvature Loss in Multimode Optic Fibres, J. Opt. Soc. Am. **71**, 12 1981.

- [10] P. Fuhr, Measuring with Light Part 1: The Physics of Fiber Optics, Sensors Magazine, 2000.
- [11] J. Hayes, Fiber Optics Technician Manual, 2000.
- [12] K. Fidanboyly and H. S. Efendioglu, Fibre Optic Sensors and their applications, 5th International Advanced Technologies Symposium, 2009.
- [13] <http://www.fibercore.com/LinkClick.aspx?fileticket=yMnVzxCwFsQ%3D&tabid=77>
- [14] Uses of Optical Fibres,
<<http://library.thinkquest.org/C006694F/Optical%20Fibres/Uses%201.htm>>, (2012, February 02).
- [15] Overview of Fiber Optic Sensors,
<http://www.bluerr.com/images/Overview_of_FOS2.pdf>, (2012, February 03)
- [16] W. A. Gambling, A. H. Hartog and C. M. Ragdale, Optical fibre transmission lines, The Rad. and Elec. Engr. **51**, 7/8 1981.
- [17] E. Ientilucci, Fundamentals of Fiber Optics, 1993.
- [18] The Basics of Fiber Optic Cable, <www.arcelect.com/fibrecable.htm>, (2011, November 24). Brief overview of fiber optic cable advantages over copper.
- [19] A. Ghatak, K. Thyagarasan, Fundamentals of Photonics, Department of Physics, Indian Institute of Technology New Delhi, India, 2000.

- [20] Attenuation, <<http://www.ofsoptics.com/resources/Understanding-Attenuation.pdf>>, (2011, October 16). Understanding Fiber Optics.
- [21] Attenuation, <<http://www.tpub.com/neets/tm/106-14.htm>>, (2011, November 03).
- [22] Measure light intensity using Light Dependant Resistor, <www.emant.com/316002.page> (2012, February 09).
- [23] D. Gloge, Bending Loss in Multimode Fibers with Graded and Ungraded Core Index, Appl. Opt. **11**,11 1972.
- [24] D. Marcusse, Losses and Impulse Response of a Parabolic Index Fiber with Random Bends, B. S. T. J. **52**, 8 1973.
- [25] W. B. Gardner, Microbending Loss in Optical Fibres, The. Be. Tech. J. **54**, 2 1974.
- [26] J. P. Quino and M. N. Confesor, Power Loss due to Macrobending in an Optical Fiber, 2005.
- [27] D. Bernhard and D. R. Velasquez, Bending Over Backwards, Corning, 2007.
- [28] S. R. Bickham, S. C. Garner, O. Kogan and T. A. Hanson, Theoretical and Experimental Studies of Macrobend losses in Multimode fibers, International Wire and Cable Symposium, Proceedings of the 58th IWCS.
- [29] Measure light intensity using Light Dependant Resistor, <www.emant.com/316002.page> (2012, February 09).

ACRONYMS and ABBREVIATIONS

EM	Electromagnetic
FOG	Fibre Optic Gyroscope
LAN	Local Area Network
LDR	Light Dependant Resistor
LED	Light Emitting Diode
MMF	Multimode Fibre
NA	Numerical Aperture
OTDR	Optical Time-Domain Reflectometer
PMMA	Polymethyl Methacrytale
POF	Plastic Optic Fibre
SMF	Single mode Fibre
TIR	Total Internal Reflection

APPENDICES

Appendix 1: Phototransistor 1 response raw results

Distance(cm)	V (mV)	V (mV)	V (mV)	AVG (mV)
34	55	54.8	54.9	54.90
29	54.7	54.6	54.8	54.70
24	54.6	54.5	54.7	54.60
20	53.9	54.1	53.8	53.93
16	53.8	53.7	53.6	53.70
12	50.1	50.3	50.2	50.20
8	50.1	50	50.2	50.10
6	34.7	34.6	34.9	34.73
4	41.7	41.5	41.4	41.53
3	51.2	51.1	51	51.10
2	49.7	49.7	49.4	49.60
1	45.3	45.4	45.4	45.37
0	42.6	42.6	42.5	42.57

Appendix 2: Phototransistor 2 response raw results

Distance (cm)	V (mV)	V (mV)	V (mV)	AVG (mV)
34	55.0	55.0	54.9	54.97
29	54.7	54.8	54.7	54.73
24	54.9	54.8	54.7	54.80
20	55.0	54.8	55.0	54.93
16	54.8	55.0	54.9	54.90
12	55.0	55.1	55.2	55.10
8	55.7	55.5	55.6	55.60
6	55.7	55.7	55.6	55.67
4	56.1	56.0	56.0	56.03
3	56.1	56.3	56.2	56.20
2	57.2	57.0	56.9	57.03
1	58.3	58.2	58.5	58.33
0	64.6	64.5	64.5	64.53

Appendix 3: LDR Response raw results

Distance (cm)	V(V)	V(V)	V(V)	Avg (V)
34	-2.85	-2.84	-2.83	-2.840
29	-2.04	-2.05	-2.04	-2.043
24	-1.27	-1.27	-1.26	-1.267
20	-0.27	-0.27	-0.27	-0.270
16	0.93	0.92	0.93	0.927
12	2.24	2.24	2.25	2.243
8	3.65	3.65	3.65	3.650
6	4.17	4.17	4.17	4.170
4	4.93	4.93	4.93	4.930
3	5.05	5.05	5.05	5.050
2	5.47	5.47	5.47	5.470
1	5.69	5.69	5.69	5.690
0	5.81	5.81	5.81	5.810

Appendix 4: Current Voltage Characteristics of LDR

Voltage (V)	Current (A)
11.910	0.010
11.500	0.020
11.200	0.025
10.520	0.030
10.030	0.040
8.880	0.050
8.190	0.060
6.790	0.070
6.580	0.075
5.190	0.090

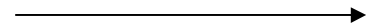
Appendix 5: Bend Diameter Measurements

Cylinder	Diameter (cm)				Average Diameter (cm)
1	1.93	1.92	1.91	1.91	1.918
2	2.14	2.15	2.14	2.16	2.148
3	2.82	2.82	2.82	2.82	2.820
4	3.33	3.32	3.32	3.34	3.328
5	4.19	4.18	4.18	4.19	4.185
6	5.11	5.11	5.11	5.09	5.105
7	6.52	6.52	6.45	6.5	6.498
8	7.39	7.4	7.43	7.41	7.408
9	10.02	10.03	9.98	10.04	10.018

Appendix 6: Measurements for the single mode fibre

		V_s (V)	$R_3(\Omega)$	$R_2/(R_1+R_2)(\Omega)$		
		12	12000	0.5		
Bend Diameter	Voltage (V) \longrightarrow				Avg V (V)	$R_x (\Omega)$
0	4.62	4.63	4.63	4.62	4.63	92727.3
9	4.90	4.90	4.90	4.90	4.90	118909.1
8	4.95	4.95	4.95	4.95	4.95	125142.9
7	5.04	5.04	5.03	5.02	5.03	136837.2
6	5.14	5.12	5.12	5.14	5.13	153517.2
5	5.20	5.18	5.19	5.20	5.19	166328.2
4	5.26	5.26	5.26	5.26	5.26	182594.6
3	5.34	5.31	5.33	5.34	5.33	202925.4
2	5.4	5.42	5.44	5.44	5.43	238434.8
1	5.61	5.62	5.63	5.63	5.62	369457.0
Input Value	4.01	4.04	4.02	3.99	4.015	60544.08

Appendix 7: Measurements for the multimode fibre

Bend Diameter(cm)	Voltage (V) 				Avg V (V)	R _x (Ω)
0	5.95	5.95	5.96	5.97	5.958	3376235.294
9	5.97	5.96	5.97	5.97	5.968	4418769.231
8	5.97	5.97	5.97	5.97	5.970	4788000.000
7	5.97	5.97	5.98	5.97	5.973	5224363.636
6	5.97	5.97	5.97	5.98	5.973	5224363.636
5	5.97	5.98	5.98	5.97	5.975	5748000.000
4	5.98	5.97	5.97	5.98	5.975	5748000.000
3	5.98	5.97	5.97	5.97	5.973	5224363.636
2	5.97	5.97	5.98	5.98	5.975	5748000.000
1	5.97	5.98	5.97	5.97	5.973	5224363.636
Input Value	4.01	4.04	4.02	3.99	4.015	60544.0806